

Two-loop corrections for nuclear matter in the Walecka model

R. J. Furnstahl

Department of Physics and Astronomy, University of Maryland, College Park, Maryland 20742

Robert J. Perry

Department of Physics, The Ohio State University, Columbus, Ohio 43210

Brian D. Serot

Physics Department and Nuclear Theory Center, Indiana University, Bloomington, Indiana 47405

(Received 8 February 1989)

Two-loop corrections for nuclear matter, including vacuum polarization, are calculated in the Walecka model to study the loop expansion as an approximation scheme for quantum hadrodynamics. Criteria for useful approximation schemes are discussed, and the concepts of strong and weak convergence are introduced. The two-loop corrections are evaluated first with one-loop parameters and mean fields and then by minimizing the total energy density with respect to the scalar field and refitting parameters to empirical nuclear matter saturation properties. The size and nature of the corrections indicate that the loop expansion is not convergent at two-loop order in either the strong or weak sense. Prospects for alternative approximation schemes are discussed.

I. INTRODUCTION

The Schrödinger equation has been a useful tool in nuclear physics for more than 50 years. Nevertheless, the existing experimental initiatives and newly completed facilities (IUCF, CEBAF, RHIC, KAON, . . .) will force us to go beyond the Schrödinger equation to compare calculations with the data of the future. A complete treatment of hadronic systems should include relativistic motion of the nucleons, dynamical mesons and baryon resonances, modifications of the nucleon structure in the nucleus, and the dynamics of the quantum vacuum, while maintaining general properties of quantum mechanics, covariance, gauge invariance, and causality. These physical effects will be relevant regardless of the degrees of freedom used to describe the system. They must be studied simultaneously and consistently if we are to draw definite conclusions about nuclear dynamics at short distances and high energies. One way to do this, at least in principle, is to use renormalizable relativistic quantum field theory based on mesons and baryons, which is known as quantum hadrodynamics (QHD).^{1,2}

QHD is a consistent framework for studying all of the physics discussed above. Here we mean that the dynamical assumptions (such as the relevant degrees of freedom, the form of the Lagrangian, and the normalization conditions) are made at the outset, and one then attempts to extract concrete results from the implied formalism. In principle, the assumptions permit the formulation of systematic, "conserving" approximations^{3,4} that maintain general physical properties. Calculations can then be compared to data to see if the framework is related to the real world and to decide where QHD succeeds and where it fails.

In QHD models with renormalizable Lagrangians, the number of parameters is finite.^{5,6} Calculations can be carried out beyond the tree level, so we can study the quantum vacuum without introducing additional parameters determined solely by short-distance phenomena. The

dynamical assumption underlying renormalizability is that the short-distance behavior and the quantum vacuum will be described in terms of hadronic degrees of freedom only. This assumption must ultimately break down, since hadrons are actually composed of quarks and gluons. However, in a renormalizable theory, all parameters can be specified using data at large distances, so that the sensitivity of calculated results to short-distance input is minimized. For QHD to be useful, nuclear observables of interest must not be dominated by contributions from short distances (where QHD is inappropriate). This conjecture must be tested by performing detailed calculations beyond the tree level.

Most of the previous work in QHD has been performed in either the mean-field theory (MFT) or at the one-loop level ("relativistic Hartree approximation" or RHA), which includes the shift in the baryon vacuum energy.^{1,7,8} The original motivation for these studies was that the MFT should become increasingly valid as the density increases and that the MFT and RHA could be good nonperturbative starting points for calculations at normal nuclear density. In fact, MFT and RHA calculations have been successful in describing a variety of nuclear systems and phenomena.^{2,9,10} For example, one finds a reasonable description of the bulk properties of spherical nuclei with parameters similar to those deduced from detailed fits of mesonic potentials to nucleon-nucleon scattering observables. These results have stimulated many successful phenomenological calculations that use Dirac nucleons and that are modeled after QHD.

Phenomenological successes notwithstanding, the QHD framework is hollow if it cannot make predictions that are subject to definitive experimental tests. Moreover, it is still unclear that the simple physical picture described by the MFT and RHA is an accurate starting point for systematic treatments of nuclear phenomena at ordinary densities. One advantage of the Schrödinger formalism is that systematic approximation schemes have been developed and used to produce reliable conclusions. Such schemes have yet to be developed for QHD.

Although QHD is formulated as a renormalizable quantum field theory, which provides the advantages discussed above, it is still a strong-coupling field theory. Unlike QCD, QHD is not asymptotically free, so most existing lattice techniques (which rely on asymptotic freedom) cannot be used.¹¹ Moreover, unlike QED, the QHD couplings are large, and there is no obvious asymptotic expansion to use to obtain results and refine them systematically. It is thus unknown whether QHD permits *any* expansion for systematic computation and refinement of theoretical results. Such an expansion (or expansions) must be found if we are to compute reliably and make definitive comparisons with precision experimental data. Our purpose in this paper is to investigate the loop expansion as a candidate for performing reliable calculations in QHD.

The loop expansion can be derived from the exact path integral of a QHD theory.^{12–18} This path integral can be used to construct an effective action^{19–25} that can be expanded order by order in loops. The effective action is a functional of the meson fields; when it is extremized with respect to the fields, it becomes proportional to the energy density of the system.^{26–28} The extremization of the effective action generates contributions to the energy density that contain the coupling constants to all orders. Thus the loop expansion is inherently *nonperturbative*. Nevertheless, this expansion places primary importance on the mean fields, and only mean fields are included nonperturbatively; all correlations, both long-range and short-range, are included perturbatively. It is therefore unlike the expansion schemes used in traditional nuclear physics, and it is of interest to see if it provides a useful procedure in QHD.

As in any quantum field theory, the QHD parameters must be specified by requiring that calculations reproduce certain empirical data. However, unlike the electron charge and mass in QED, the QHD couplings and some of the masses cannot be directly measured experimentally. These parameters must be inferred from “higher-level” data, such as nucleon-nucleon scattering observables or the properties of nuclei. Since the calculated expressions for these higher-level observables change as one refines the calculations, forcing a readjustment of the parameters, it is crucial to define the characteristics of reliable expansions in a strong-coupling theory.

The most important feature of a useful expansion is that corrections get smaller as one proceeds to higher orders. This does not necessarily imply mathematical convergence; recall that QED expansions in α are only asymptotic. The crucial point is that the QED expansion procedure is robust enough to generate results whose precision matches or exceeds that of the experimental data. Useful expansion procedures in QHD must have similar capabilities.

Since QHD contains strong couplings, it is highly unlikely that any expansion will converge in the mathematical sense. Moreover, a straightforward expansion in the couplings is not even asymptotic, as in QED. In this paper, we will use the term “convergent” not in the strict sense, but rather to imply that the terms in an expansion decrease in magnitude as one proceeds to higher and

higher orders. We consider three types of useful expansions. The first is a *perturbative* expansion, which is carried out order by order in the coupling constants around some initial (zeroth-order) approximation that may be nonperturbative. Correction terms are evaluated *using parameters and mean fields determined in the previous order*. If the correction terms are (relatively) small, the perturbative expansion is useful.

In contrast, we define two types of nonperturbative expansions. A nonperturbative expansion is *strongly convergent* if it satisfies two criteria: First, there is a systematic procedure for computing all terms in the expansion, at least in principle. Second, if the couplings and masses are determined at a given order, the next term in the expansion is small when evaluated with the same parameters. For example, in the loop expansion, this implies that mean fields must still be determined in each order by extremizing the effective action, which is a nonperturbative procedure. This may be contrasted with the perturbative expansion, where the corrections are computed with the lower-order parameters *and* mean fields.

In the second type of nonperturbative expansion, results are evaluated at two successive orders, and the model parameters are adjusted at each order to reproduce the normalization conditions. If the corrections computed in this way are (relatively) small, the expansion is *weakly convergent*. This is a more subjective criterion, since we must also require, in some way that is not precisely defined, that calculated results do not change qualitatively from one order to the next. In particular, the readjustment of parameters should not produce drastic changes in the parameter values or in the basic features of the implied nucleon-nucleon interaction.

In a hadronic relativistic field theory, weakly convergent expansions are more natural than strongly convergent expansions for the following reason. The calculation of corrections always involves the removal of divergences and subsequent renormalization of parameters. The finite parameter values are determined through normalization conditions that must be satisfied in any physically relevant approximation. Unlike QED, where the physical electron mass and charge can be measured classically, some of the QHD masses and couplings are not directly measurable. In practice, the normalization conditions in QHD typically involve experimental quantities described by complicated functions of the *renormalized* parameters that are known only at the current level of calculation. Since the couplings are strong, the deduced values of some parameters will change when the calculations are carried to the next order. Thus it is somewhat unnatural to define the renormalization to maintain the parameters at their lower-order values, as required in a strongly convergent expansion.

The calculations in the present paper are based on the seminal works of Coleman and Weinberg²² and Lee and Wick,²⁸ together with their recent application to QHD in Refs. 29–31. Similar calculations have been performed by a number of authors. For example, Lee and Margulies studied a weak-coupling, high-density loop expansion in the linear σ model,^{32,33} including all of the two-loop terms and the dominant three-loop contributions. Their

emphasis, however, was on the development of a chirally symmetric renormalization scheme, which leads to very complicated expressions for the loop integrals.³³ Moreover, Lee and Margulies did not perform any quantitative calculations appropriate for nuclear matter. Nyman and Rho also studied the loop expansion in the σ model^{34,35} by considering a subset of the one- and two-loop diagrams. These authors emphasized the large scale of the one-loop vacuum corrections, but argued that the corrections could be reduced by an appropriate choice of the scalar mass. (Two-loop vacuum corrections were ignored.) As they were primarily concerned with the properties of “abnormal” nuclear matter,²⁸ Nyman and Rho did not present numerical results for the normal state. Jackson, Rho, and Krotschek³⁶ extended the σ -model calculations to normal nuclear matter, but included only a subset of the two-loop contributions and evaluated them approximately. To our knowledge, no previous calculations have included fluctuations from *both* scalar and vector fields. In particular, two-loop fluctuation contributions to the energy are absent in the relativistic electron gas;³⁷ an additional scalar field is necessary to shift the fermion mass and produce nonzero fluctuations from photon exchange.

In contrast to the previous analyses, we consider the Walecka model, with Lagrangian density given by Eq. (2.42). This model contains some basic elements of hadronic theories of nuclei, namely, baryons coupled strongly to neutral scalar and vector fields. Consistent with the philosophy of QHD, both of these mesons are treated as true quantum degrees of freedom. Our emphasis is not on quantitative accuracy in describing experiment, but rather on the formulation and investigation of reliable approximation schemes in strong-coupling relativistic quantum field theory. We will measure our success by examining the stability of predictions for physical observables.

We derive an exact expression for the ground-state to ground-state generating functional that can be expanded to any order in loops. In this paper, we compute terms at one- and two-loop order in infinite nuclear matter. The two-loop contributions to the energy density are shown in Fig. 1, and the full two-loop corrections, including vacuum polarization, are calculated exactly. Both of the two-loop diagrams are infinite and contain nested and overlapping divergences. The renormalization of these diagrams is discussed in Sec. II. We evaluate the two-

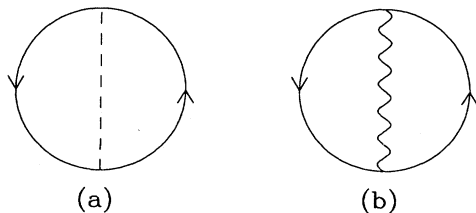


FIG. 1. Two-loop contributions to the nuclear matter energy density. The solid line represents the baryon propagator, and the dashed and wiggly lines denote scalar and vector mesons, respectively. Counterterm contributions and vacuum subtractions, which are necessary to produce finite results, are not shown.

loop contributions using the RHA (one-loop) parameters to see if the loop expansion is perturbatively or strongly convergent. We also determine new couplings and masses for the two-loop calculation by minimizing with respect to the scalar field and normalizing to the empirical binding energy and equilibrium density of nuclear matter. This tests weak convergence. To our knowledge, this is the first two-loop calculation in a hadronic field theory that includes the mean fields to all orders and that uses parameters that reproduce nuclear matter saturation properties.

Through two-loop order, the loop expansion for the Walecka model is neither perturbatively nor strongly convergent. For example, in a perturbative calculation using the RHA parameters and mean fields, the two-loop corrections are huge: nuclear matter saturates at a Fermi momentum of 2 fm^{-1} with a binding energy of 400 MeV/nucleon. Moreover, the scalar field that minimizes the two-loop energy density leads to an unphysical solution at equilibrium nuclear density. This behavior persists as the density is increased. Thus the validity of the MFT at high density becomes a subtle question that we discuss in Sec. IV.

It is possible to find parameter sets that reproduce nuclear saturation at the two-loop level. With the new parameters, the resulting nuclear binding curves are similar to the one-loop result. Nevertheless, the qualitative features of the description are very different from the RHA because the parameters must be tuned to minimize corrections from the quantum vacuum at the two-loop level. In particular, two-loop terms involving vector mesons (which have never been studied before) are too attractive for values of the vector coupling used in all previous QHD studies and values implied by modern boson-exchange potentials. After fine tuning, nuclear matter saturation is achieved almost entirely from the dynamics of scalar-meson exchange—in particular, from an interplay of attractive one-loop terms and repulsive scalar two-loop terms that involve occupied states in the Fermi sea. In fact, it is possible to reproduce nuclear matter saturation with no vector meson at all. These qualitative changes lead us to conclude that the two-loop contributions produce large corrections to the RHA results. The loop expansion (through two-loop order) is not even weakly convergent.

The outline of this paper is as follows. In Sec. II, we describe the loop expansion and derive the formal (unrenormalized) expressions for the two-loop corrections to the energy. We then discuss the renormalization procedure and generate finite expressions that are used in our numerical calculations. Results for both perturbative and nonperturbative calculations are given in Sec. III. Section IV considers the implications of our results in the context of QHD and summarizes our conclusions. Various technical details are included in the Appendixes. As Secs. III and IV are reasonably self-contained, readers who are not interested in the formal developments may find it useful to skip Sec. II.

II. FORMALISM

In this section we consider the loop expansion as a systematic procedure for calculating in QHD. We start with

the exact ground-state to ground-state generating functional of the theory, which is written as a path integral. This path integral is used to define an effective action, which is the field-theoretic analog of the Helmholtz free energy in statistical mechanics.²⁸ The effective action can be expanded systematically around its classical value by considering terms with increasing numbers of quantum loops. The “loop expansion” is formally a power series in \hbar , but as pointed out by several authors,^{22,25–27} \hbar is merely a bookkeeping parameter and need not be considered “small.” In fact, as we will show, the loop expansion is a perturbative expansion in powers of the coupling constants using a propagator that is defined nonperturbatively.

We will review the basic ideas of the effective action formalism and loop expansion for a self-interacting scalar field theory²⁵ and then generalize to the Walecka model. Although some of this material can be found scattered through the literature, we repeat it here in an organized fashion to coherently develop several new aspects and to allow our results to be verified by other investigators.

A. Scalar fields

Consider a real scalar field described by the Lagrangian density

$$\mathcal{L}(x) = \frac{1}{2}[\partial_\mu \phi(x) \partial^\mu \phi(x) - m_s^2 \phi^2(x)] - V(\phi(x)) + \delta \mathcal{L} \quad (2.1)$$

and action

$$S[\phi] \equiv \int d^4x \mathcal{L}(\phi(x), \partial_\mu \phi(x)) \equiv \int d^4x \mathcal{L}(x) . \quad (2.2)$$

The counterterms contained in $\delta \mathcal{L}$ will be written explicitly when needed. The classical value ϕ_0 of the scalar field occurs at the minimum of the potential $U(\phi) = \frac{1}{2} m_s^2 \phi^2 + V(\phi)$, which we assume is at $\phi_0 = 0$.

In contrast, the vacuum expectation value of the quantum field, which we denote by $\bar{\phi}$, is defined by

$$\bar{\phi} \equiv \lim_{j \rightarrow 0} \frac{\langle 0^+ | \hat{\phi} | 0^- \rangle_j}{\langle 0^+ | 0^- \rangle_j} . \quad (2.3)$$

Here $\hat{\phi}$ is the scalar field operator and $\langle 0^+ | 0^- \rangle_j$ is the vacuum-to-vacuum amplitude in the presence of an external classical source $j(x)$. Since $\bar{\phi}$ is distinct from ϕ_0 , we may find that $\bar{\phi} \neq 0$.

The generating functional $Z[j]$ and connected generating functional $W[j]$ are defined by the path integral^{2,15}

$$\begin{aligned} Z[j] &\equiv \exp(iW[j]/\hbar) \\ &\equiv \mathcal{N} \int D(\phi) \exp \left[\frac{i}{\hbar} \int d^4x [\mathcal{L}(x) + j(x)\phi(x)] \right] , \end{aligned} \quad (2.4)$$

$$\mathcal{N}^{-1} \equiv \int D(\phi) \exp \left[\frac{i}{\hbar} \int d^4x \mathcal{L}(x) \right] , \quad (2.5)$$

where \hbar has been indicated explicitly. Since the scalar theory defined above is canonical, Eq. (2.4) can be derived by first writing a path integral over the scalar field and its conjugate momentum^{15–17} and then performing the

Gaussian momentum integrals; this also generates various normalization factors,³⁸ which are canceled by \mathcal{N} . Since the spacetime integrals are written in Minkowski space, we shift the scalar mass by an infinitesimal ($m_s^2 \rightarrow m_s^2 - i\eta$) to define the path integral. (Alternatively, we could begin with a Euclidean path integral defined at finite temperature T and consider the desired generating functional as the $T \rightarrow 0$ limit.³⁹)

$W[j]$ generates all totally connected n -point amplitudes and is a functional of the external source j . For any j , there is a corresponding expectation value

$$\phi_e(x) \equiv \frac{\langle 0^+ | \hat{\phi}(x) | 0^- \rangle_j}{\langle 0^+ | 0^- \rangle_j} = -i\hbar \frac{\delta \ln Z[j]}{\delta j(x)} = \frac{\delta W[j]}{\delta j(x)} \quad (2.6)$$

that reduces to the vacuum result for a vanishing source:

$$\lim_{j \rightarrow 0} \phi_e(x) = \bar{\phi} = \text{const} . \quad (2.7)$$

Suppose, however, that we want to find the source that produces a particular $\phi_e(x)$. This requires a reformulation of the problem so that ϕ_e is the independent variable, which is achieved through a functional Legendre transformation.²⁰ Define the effective action $\Gamma[\phi_e]$ by

$$\Gamma[\phi_e] \equiv W[j] - \int d^4x j(x)\phi_e(x) , \quad (2.8)$$

where $j(x)$ is to be eliminated in favor of $\phi_e(x)$ by solving Eq. (2.6). This transformation ensures that $\Gamma[\phi_e]$ is independent of j ,

$$\frac{\delta \Gamma[\phi_e]}{\delta j(x)} = 0 . \quad (2.9)$$

Moreover, functional differentiation with respect to ϕ_e and the use of Eq. (2.6) produces

$$\frac{\delta \Gamma[\phi_e]}{\delta \phi_e(x)} = -j(x) . \quad (2.10)$$

If we set $j = 0$, ϕ_e must become a constant, equal to the vacuum expectation value, which implies

$$\left[\frac{\delta \Gamma[\phi_e]}{\delta \phi_e} \right]_{\phi_e = \bar{\phi}} = 0 . \quad (2.11)$$

Thus the vacuum expectation value $\bar{\phi}$ is obtained by extremizing the effective action with respect to ϕ_e .

The effective action can be interpreted by expanding it in a functional Taylor series:

$$\begin{aligned} \Gamma[\phi_e] &= \sum_{n=2}^{\infty} \frac{1}{n!} \int d^4x_1 \cdots d^4x_n \Gamma_n(x_1, \dots, x_n) \\ &\quad \times \phi_e(x_1) \cdots \phi_e(x_n) . \end{aligned} \quad (2.12)$$

Here we have assumed that $\Gamma[0] = 0$ is an extremum, which can be enforced by appropriate renormalization conditions.^{2,25} It can be shown^{18,20,23,25,26} that Γ_n consists of all proper n -point vertices, that is, the sum of all closed, connected, one-particle irreducible (1-PI) Feynman diagrams with n amputated external legs. If we now demand [see Eq. (2.11)] that

$$\begin{aligned} \frac{\delta\Gamma[\phi_e]}{\delta\phi_e(y)} &= \sum_{n=2}^{\infty} \frac{1}{(n-1)!} \int d^4x_1 \cdots d^4x_{n-1} \\ &\quad \times \Gamma_n(x_1, \dots, x_{n-1}, y) \phi_e(x_1) \cdots \phi_e(x_{n-1}) \\ &= 0, \end{aligned} \quad (2.13)$$

we obtain an *implicit equation* for the vacuum expectation value $\bar{\phi}$. The solution to this equation expresses $\bar{\phi}$ in terms of all the 1-PI vertices with $n \geq 2$. It now follows from Eq. (2.12) that when we evaluate $\Gamma[\phi_e = \bar{\phi}]$, we connect strings of 1-PI vertices to the external sites of each Γ_n . Thus $\Gamma[\phi_e = \bar{\phi}]$ contains all closed, connected diagrams in the theory, both reducible and irreducible. When the calculation is carried out to a given order in loops, the extremization of $\Gamma[\phi_e]$ ensures that the mean field $\bar{\phi}$ is calculated using all diagrams with the desired number of internal loops.

For application to infinite matter, it is most convenient to expand the effective action in powers of derivatives of the field:²⁵

$$\Gamma[\phi] = \int d^4x \left[-U_{\text{eff}}(\phi) + \frac{1}{2} Z_{\text{eff}}(\phi) (\partial^\mu \phi)^2 + \cdots \right]. \quad (2.14)$$

The first term gives the sum of all 1-PI vertices connected to ϕ fields at zero external momenta, while the remaining

terms involve nonzero momentum components. Thus, if we consider *uniform* fields $\bar{\phi}$, only the first term remains, and the effective potential U_{eff} is proportional to the effective action:

$$\Gamma[\bar{\phi}] = - \int d^4x U_{\text{eff}}(\bar{\phi}). \quad (2.15)$$

We now illustrate these ideas for the theory described by Eq. (2.1). As much of this material exists in the literature (see, for example, Ref. 25 or Chap. 6 of Ref. 2), the discussion here will be brief. Begin by expanding the exponent in Eq. (2.4) about a classical field ϕ_0 that makes the action (2.2) stationary in the presence of an external source $j(x)$. This field satisfies

$$\begin{aligned} - \left[\frac{\delta S[\phi]}{\delta \phi(x)} \right]_{\phi=\phi_0} &= (\partial^2 + m_s^2) \phi_0(x) + V'(\phi_0(x)) \\ &= j(x), \end{aligned} \quad (2.16)$$

and we can expand in the quantum fluctuations about this field by defining

$$\phi(x) \equiv \phi_0(x) + \hbar^{1/2} \sigma(x). \quad (2.17)$$

In this way, the generating functional (2.4) can be written as

$$\begin{aligned} Z[j] &= \mathcal{N} \exp \left[\frac{i}{\hbar} \left[S[\phi_0] + \int d^4x j(x) \phi_0(x) \right] \right] \int D(\sigma) \exp \left[\frac{i}{2} \int d^4x \sigma \left[-\partial^2 - m_s^2 - V'''(\phi_0) \right] \sigma \right] \\ &\quad \times \exp \left[-i \sum_{n=3}^{\infty} \frac{\hbar^{(n-2)/2}}{n!} \int d^4x \sigma^n V^{(n)}(\phi_0) \right], \end{aligned} \quad (2.18)$$

where

$$S[\phi_0] \equiv \int d^4x \left[\frac{1}{2} \phi_0 (-\partial^2 - m_s^2) \phi_0 - V(\phi_0) \right] \quad (2.19)$$

and $V^{(n)}(\phi_0) \equiv d^n V / d\phi_0^n$. We have also let $\phi \rightarrow \hbar^{1/2} \phi$ in the definition of \mathcal{N} [Eq. (2.5)], which cancels the factor of \hbar in the exponent.

To perform the functional integral over σ , we remove the final exponential factor in Eq. (2.18) by introducing an auxiliary source $u(x)$ that couples to $\sigma(x)$ and that must be set to zero before performing the Legendre transformation (2.8). This allows us to write

$$\begin{aligned} Z[j; u] &= \mathcal{N} \exp \left[\frac{i}{\hbar} \left[S[\phi_0] + \int d^4x j(x) \phi_0(x) \right] \right] \exp \left[-i \sum_{n=3}^{\infty} \frac{\hbar^{(n-2)/2}}{n!} \int d^4x V^{(n)}(\phi_0) \left[\frac{-i\delta}{\delta u} \right]^n \right] \\ &\quad \times \int D(\sigma) \exp \left[i \int d^4x \left\{ \frac{1}{2} \sigma \left[-\partial^2 - m_s^2 - V'''(\phi_0) \right] \sigma + u \sigma \right\} \right]. \end{aligned} \quad (2.20)$$

This expression is still exact but plagued by ultraviolet divergences that will be discussed below.

The remaining Gaussian path integral can be performed easily, as shown in numerous texts.^{2,15-18} Note that the normalization constant defined in Eq. (2.5) serves two purposes: it cancels various factors arising from the path-integral measure, and it also provides a subtraction of pure vacuum diagrams. To see how this works, define

$$I_V(u) \equiv \int D(\sigma) \exp \left[i \int d^4x \left\{ \frac{1}{2} \sigma \left[-\partial^2 - m_s^2 - V'''(\phi_0) \right] \sigma + u \sigma \right\} \right]. \quad (2.21)$$

If we now assume *uniform* classical fields, this integral can be expressed in the compact form

$$I_V(u) = I_0(0) \exp \left[-\frac{1}{2} \int d^4x \int \frac{d^4k}{(2\pi)^4} \ln \left[1 - \frac{V'''(\phi_0)}{k^2 - m_s^2 + i\eta} \right] \right] \exp \left[-\frac{i}{2} \int d^4x d^4y u(x) \Delta(x-y) u(y) \right], \quad (2.22)$$

where $I_0(u)$ is the path integral of Eq. (2.21) with $V'''=0$, and $\Delta(x-y)$ is the scalar propagator in the presence of the classical field ϕ_0 :

$$\Delta(x-y) = \int \frac{d^4k}{(2\pi)^4} e^{-ik(x-y)} \frac{1}{k^2 - m_s^2 - V''(\phi_0) + i\eta}. \quad (2.23)$$

With these results, we can rewrite Eq. (2.20) as

$$\begin{aligned} Z[j] = & \mathcal{N}' \exp \left[\frac{i}{\hbar} \left[S[\phi_0] + \int d^4x j \phi_0 \right] \right] \exp \left[-\frac{1}{2} \int d^4x \int \frac{d^4k}{(2\pi)^4} \ln \left[1 - \frac{V''(\phi_0)}{k^2 - m_s^2 + i\eta} \right] \right] \\ & \times \left\{ \exp \left[-i \sum_{n=3}^{\infty} \frac{\hbar^{(n-2)/2}}{n!} \int d^4z V^{(n)}(\phi_0) \left[\frac{-i\delta}{\delta u(z)} \right]^n \right] \exp \left[-\frac{i}{2} \int d^4x d^4y u(x) \Delta(x-y) u(y) \right] \right\}_{u=0}. \end{aligned} \quad (2.24)$$

The new normalization factor is

$$\begin{aligned} \mathcal{N}' \equiv I_0(0), \mathcal{N} = I_0(0) & \left\{ \exp \left[-i \sum_{n=3}^{\infty} \frac{\hbar^{(n-2)/2}}{n!} \int d^4z V^{(n)}(0) \left[\frac{-i\delta}{\delta u(z)} \right]^n \right] I_0(u) \right\}_{u=0}^{-1} \\ & = \left\{ \exp \left[-i \sum_{n=3}^{\infty} \frac{\hbar^{(n-2)/2}}{n!} \int d^4z V^{(n)}(0) \left[\frac{-i\delta}{\delta u(z)} \right]^n \right] \exp \left[-\frac{i}{2} \int d^4x d^4y u(x) \Delta^0(x-y) u(y) \right] \right\}_{u=0}^{-1}, \end{aligned} \quad (2.25)$$

which is obtained by expanding (2.5) about the *vacuum* classical field $\phi_0=0$ and incorporating the factor of I_0 from Eq. (2.22). [We assume that $V(\phi)$ is at least cubic in ϕ .] Δ^0 is the noninteracting scalar propagator obtained by setting $V''=0$ in Eq. (2.23). Equation (2.24) is still exact for uniform ϕ_0 and includes all vacuum-to-vacuum diagrams in the presence of an external source j . The factor \mathcal{N}' removes all such diagrams that would exist even in the absence of the source, thus providing an overall normalization.

Since the \hbar factors are explicit in Eq. (2.24), we identify the first exponential as the classical contribution, the second as the one-loop quantum correction, and the final two as generating higher-order loop corrections. A systematic expansion in powers of \hbar thus generates the loop expansion for this interacting scalar field theory and allows the effects of virtual particles to be included consistently. We emphasize that Eq. (2.24) is valid only for uniform classical fields; the generalization to spatially varying fields is straightforward, but messy. It is then usually most efficient to expand the functional as a power series in derivatives of the classical field.^{25,40-44}

We now consider the removal of divergences in the loop expansion and specialize to renormalizable self-couplings:

$$V(\phi) = \frac{1}{3!} \kappa \phi^3 + \frac{1}{4!} \lambda \phi^4. \quad (2.26)$$

Begin by working to one-loop order. By comparing Eq. (2.24) to the definition of the connected generating functional in Eq. (2.4), we find

$$W^{(1)}[j] = \int d^4x \left[\frac{1}{2} \phi_0 (-\partial^2 - m_s^2) \phi_0 + j \phi_0 - V(\phi_0) - \frac{\hbar}{2i} \int \frac{d^4k}{(2\pi)^4} \ln \left[1 - \frac{V''(\phi_0)}{k^2 - m_s^2 + i\eta} \right] \right]. \quad (2.27)$$

This is indeed a functional of j , since $\phi_0 = \phi_0[j]$ through Eq. (2.16). To construct the effective action $\Gamma[\phi_e]$, we must rewrite (2.27) in terms of ϕ_e . At this order, however, the Legendre transformation is trivial, since $\phi_e - \phi_0 \sim \mathcal{O}(\hbar)$, and the classical action (including the source term) is stationary about ϕ_0 . Thus we may simply replace ϕ_0 by ϕ_e in Eq. (2.27) and eliminate the $j\phi_0$ term to arrive at the one-loop effective action

$$\Gamma^{(1)}[\phi_e] = \int d^4x \left[\frac{1}{2} \phi_e (-\partial^2 - m_s^2) \phi_e - V(\phi_e) + \frac{i\hbar}{2} \int \frac{d^4k}{(2\pi)^4} \ln \left[1 - \frac{V''(\phi_e)}{k^2 - m_s^2 + i\eta} \right] \right]. \quad (2.28)$$

To complete the analysis, we must remove the ultraviolet divergences in the integral over k . This is accomplished by introducing $\mathcal{O}(\hbar)$ counterterms of the form

$$\delta\mathcal{L}^{(1)} = \hbar \left[\bar{\alpha}_1^{(1)} \phi + \frac{1}{2!} \bar{\alpha}_2^{(1)} \phi^2 + \frac{1}{3!} \bar{\alpha}_3^{(1)} \phi^3 + \frac{1}{4!} \bar{\alpha}_4^{(1)} \phi^4 \right] \quad (2.29)$$

into the Lagrangian of Eq. (2.1). Since the \hbar has been factored out to facilitate power counting, the superscript (1) will remind us that these counterterms entered at one-loop order. (The bar distinguishes these counterterms, which renormalize scalar loops, from those introduced later, which renormalize fermion loops.)

To include the counterterms in the analysis, expand (2.29) around the classical field ϕ_0 using Eq. (2.17), producing

$$\delta\mathcal{L}^{(1)} = \hbar \sum_{n=1}^4 \frac{1}{n!} \bar{\alpha}_n^{(1)} \phi_0^n + \hbar \sum_{n=1}^4 \hbar^{n/2} a_n^{(1)} \sigma^n, \quad (2.30)$$

where

$$\begin{aligned} a_1^{(1)} &\equiv \bar{\alpha}_1^{(1)} + \bar{\alpha}_2^{(1)} \phi_0 + \frac{1}{2} \bar{\alpha}_3^{(1)} \phi_0^2 + \frac{1}{6} \bar{\alpha}_4^{(1)} \phi_0^3, & a_2^{(1)} &\equiv \frac{1}{2} \bar{\alpha}_2^{(1)} + \frac{1}{2} \bar{\alpha}_3^{(1)} \phi_0 + \frac{1}{4} \bar{\alpha}_4^{(1)} \phi_0^2, \\ a_3^{(1)} &\equiv \frac{1}{6} \bar{\alpha}_3^{(1)} + \frac{1}{6} \bar{\alpha}_4^{(1)} \phi_0, & a_4^{(1)} &\equiv \frac{1}{24} \bar{\alpha}_4^{(1)}. \end{aligned} \quad (2.31)$$

The counterterms can now be inserted into Eq. (2.18). The σ -independent pieces are grouped with the one-loop action, and the factors of σ^n in the remaining pieces are rewritten as functional derivatives, as in Eq. (2.20), leading to

$$\begin{aligned} Z[j] &= \mathcal{N}' \exp \left[\frac{i}{\hbar} \left[S[\phi_0] + \int d^4x j \phi_0 \right] \right] \exp \left[-\frac{1}{2} \int d^4x \int \frac{d^4k}{(2\pi)^4} \ln \left[1 - \frac{V''(\phi_0)}{k^2 - m_s^2 + i\eta} \right] + i \sum_{n=1}^4 \frac{1}{n!} \bar{\alpha}_n^{(1)} \int d^4x \phi_0^n \right] \\ &\times \left[\exp \left\{ i \int d^4z \left[\sum_{n=1}^4 \hbar^{n/2} a_n^{(1)} \left[\frac{-i\delta}{\delta u} \right]^n - \hbar^{1/2} \frac{\kappa + \lambda \phi_0}{6} \left[\frac{-i\delta}{\delta u} \right]^3 - \hbar \frac{\lambda}{24} \left[\frac{-i\delta}{\delta u} \right]^4 \right] \right\} \right. \\ &\left. \times \exp \left[-\frac{i}{2} \int d^4x d^4y u(x) \Delta(x-y) u(y) \right] \right]_{u=0}. \end{aligned} \quad (2.32)$$

Thus the linear combinations of one-loop counterterms in Eq. (2.31) will enter in higher-order loop diagrams to remove internal divergences, as we will see shortly. It is also apparent that an expansion in powers of \hbar produces a perturbative expansion in the couplings κ and λ and the propagator $\Delta(x-y)$ of Eq. (2.23). Since there are only a finite number of new diagrams appearing in any order of loops, and since these differ from lower-order diagrams by finite powers of the couplings, the renormalization procedure can be extended to higher loops by adding new counterterms (of higher order in \hbar) and proceeding analogously. The closed-loop diagrams can therefore be treated exactly, without further approximation.

The σ -independent counterterm pieces are simply carried along in the exponent and appear in the one-loop effective action (2.28), after replacing $\phi_0 \rightarrow \phi_e$. Comparing this result with Eq. (2.15) allows us to deduce the renormalized one-loop effective potential

$$\begin{aligned} U_{\text{eff}}^{(1)}(\phi) &= \frac{1}{2} m_s^2 \phi^2 + V(\phi) \\ &- \frac{i\hbar}{2} \int \frac{d^4k}{(2\pi)^4} \ln \left[1 - \frac{V''(\phi)}{k^2 - m_s^2 + i\eta} \right] \\ &- \hbar \sum_{n=1}^4 \frac{\bar{\alpha}_n^{(1)}}{n!} \phi^n, \end{aligned} \quad (2.33)$$

where

$$V''(\phi) = \kappa \phi + \lambda \phi^2 / 2.$$

The renormalization conditions that define the $\bar{\alpha}_n^{(1)}$ counterterms are discussed in Ref. 2 and will not be repeated here. Of primary importance is that the counterterms are defined by vacuum diagrams with *vanishing* external momenta; this produces the simplest expression for the effective potential, which is the primary quantity of interest here. The final result for the renormalized one-loop effective potential is given in Eq. (6.76) of Ref. 2.

We turn now to the effective action at two-loop order, starting with Eq. (2.32). By evaluating the last two exponentials in this expression to $O(\hbar)$, one can identify the two-loop contributions to the connected generating func-

tional W . There are also contributions to W in this order from the normalization constant \mathcal{N}' of Eq. (2.25); these represent vacuum subtractions and are independent of j and ϕ_0 . We will denote the sum of these pieces as $W_2[\phi_0]$.

The Legendre transformation (2.8) becomes

$$\begin{aligned} \Gamma^{(2)}[\phi_e] &= S[\phi_0] + \int d^4x j(\phi_0 - \phi_e) \\ &+ W_1[\phi_0] + W_2[\phi_0] + O(\hbar^3), \end{aligned} \quad (2.34)$$

where $W_1[\phi_0]$ is the $O(\hbar)$ piece of Eq. (2.27) plus the $O(\hbar)$ counterterms, as in Eq. (2.33). The right-hand side of (2.34) (which is a functional of j) must be rewritten in terms of ϕ_e by letting $j \rightarrow j[\phi_0]$ and then changing variables from ϕ_0 to ϕ_e .

If $j \rightarrow j[\phi_0]$, Eq. (2.16) implies

$$\begin{aligned} -\frac{\delta j(x)}{\delta \phi_0(y)} &= \frac{\delta^2 S[\phi_0]}{\delta \phi_0(x) \delta \phi_0(y)} \\ &= -[\partial^2 + m_s^2 + V''(\phi_0)] \delta^{(4)}(x-y) \\ &= [\Delta(x-y)]^{-1}. \end{aligned} \quad (2.35)$$

To accomplish the change of variables from ϕ_0 to ϕ_e , let us define $\phi_0 \equiv \phi_e + \phi_1$, where ϕ_1 cancels the quantum corrections contained in ϕ_e and is at least of $O(\hbar)$.

We can now expand Eq. (2.34) about ϕ_e as a power series in ϕ_1 . To this order, we can simply replace ϕ_0 by ϕ_e in W_2 . Moreover, since $j[\phi_0]$ is determined by Eq. (2.16), the expansion of the first two terms in Eq. (2.34) has no term linear in ϕ_1 . This implies that we need only the $O(\hbar)$ contribution to ϕ_1 , which can be calculated from Eqs. (2.6), (2.27), and (2.35), with the result

$$\phi_1(x) = \int d^4y \Delta(x-y) \left[\frac{\delta W_1}{\delta \phi_0(y)} \right]. \quad (2.36)$$

This relation and those in Eq. (2.35) allow the remaining terms with ϕ_1 dependence to be combined, producing

$$\Gamma^{(2)}[\phi_e] = \Gamma^{(1)}[\phi_e] + W_2[\phi_e] + \frac{1}{2} \int d^4x d^4y \left[\frac{\delta W_1}{\delta \phi_0(x)} \right] \Delta(x-y) \left[\frac{\delta W_1}{\delta \phi_0(y)} \right] + O(\hbar^3). \quad (2.37)$$

Here $\Gamma^{(1)}[\phi_e]$ is given by Eq. (2.28) (plus counterterms), and the integrand of the double integral is to be evaluated at $\phi_0 = \phi_e$ using

$$\left[\frac{\delta W_1[\phi_0]}{\delta \phi_0} \right]_{\phi_0 = \phi_e} = -i\hbar \frac{\kappa + \lambda \phi_e}{2} \int \frac{d^4k}{(2\pi)^4} \frac{1}{k^2 - m_s^2 - V''(\phi_e) + i\eta} + \hbar a_1^{(1)}(\phi_e), \quad (2.38)$$

where $a_1^{(1)}(\phi_0)$ is given in Eq. (2.31). Since we have assumed uniform and constant fields, this last result is independent of spacetime, and its substitution into Eq. (2.37) shows that the double integral generates *one-particle reducible* contributions to $\Gamma^{(2)}$ of $O(\hbar^2)$. It can be verified that these terms *cancel* the reducible diagrams in W_2 originating from the expansion of the final two exponentials in Eq. (2.32). Moreover, reducible diagrams contained in the vacuum subtraction cancel among themselves by virtue of the definition of $\bar{\alpha}_1^{(1)}$. This cancellation of reducible diagrams persists to all orders in loops.^{18,20,23,25,26}

Thus Eq. (2.37) contains only irreducible diagrams and is valid to $O(\hbar^2)$. By comparing to Eq. (2.15), we can write the effective potential through two-loop order as

$$U_{\text{eff}}^{(2)}(\phi) = U_{\text{eff}}^{(1)}(\phi) - \hbar^2 \frac{\lambda}{8} \int \frac{d^4k}{(2\pi)^4} \Delta(k) \int \frac{d^4t}{(2\pi)^4} \Delta(t) - \hbar^2 \frac{(\kappa + \lambda \phi)^2}{12} \int \frac{d^4k}{(2\pi)^4} \frac{d^4t}{(2\pi)^4} \Delta(k) \Delta(t) \Delta(k+t) \\ - i \frac{\hbar^2}{2} (\bar{\alpha}_2^{(1)} + \bar{\alpha}_3^{(1)} \phi + \frac{1}{2} \bar{\alpha}_4^{(1)} \phi^2) \int \frac{d^4k}{(2\pi)^4} \Delta(k) - i \frac{\hbar^2}{2} \bar{\xi}_s \int \frac{d^4k}{(2\pi)^4} k^2 \Delta(k) - \hbar^2 \sum_{n=1}^4 \frac{1}{n!} \bar{\alpha}_n^{(2)} \phi^n - \text{VEV}, \quad (2.39)$$

where

$$\Delta(k) = \frac{1}{k^2 - m_s^2 - V''(\phi) + i\eta}. \quad (2.40)$$

We have included $O(\hbar^2)$ counterterms $\bar{\alpha}_n^{(2)}$ of the form in Eq. (2.29), together with a wave-function counterterm arising from

$$\delta \mathcal{L}' = \frac{\hbar}{2} \bar{\xi}_s \partial^\mu \phi \partial_\mu \phi = - \frac{\hbar^2}{2} \bar{\xi}_s \sigma \partial^2 \sigma,$$

and the vacuum expectation value (VEV) subtraction is given by

$$\text{VEV} = - \frac{i\hbar^2}{2} \bar{\alpha}_2^{(1)} \int \frac{d^4k}{(2\pi)^4} \Delta^0(k) - i \frac{\hbar^2}{2} \bar{\xi}_s \int \frac{d^4k}{(2\pi)^4} k^2 \Delta^0(k) \\ - \hbar^2 \frac{\lambda}{8} \int \frac{d^4k}{(2\pi)^4} \Delta^0(k) \int \frac{d^4t}{(2\pi)^4} \Delta^0(t) \\ - \hbar^2 \frac{\kappa^2}{12} \int \frac{d^4k}{(2\pi)^4} \frac{d^4t}{(2\pi)^4} \Delta^0(k) \Delta^0(t) \Delta^0(k+t). \quad (2.41)$$

Here $\Delta^0(k)$ is the noninteracting scalar propagator in momentum space.

We have thus illustrated how the systematic expansion of Eq. (2.32) in powers of \hbar and the subsequent Legendre transformation (2.8) of the connected generating functional W produce the loop expansion of the effective action Γ . Only one-particle irreducible contributions ap-

pear in the final result, as the minimization with respect to ϕ generates the reducible contributions to the desired order. We postpone a discussion of the renormalization of (2.39) until we derive the corresponding expression in the Walecka model and here merely state the results. After the vacuum subtraction, the first two integrals contain nested, overlapping, and overall divergences. (These are defined below.) The terms involving the $\bar{\alpha}_n^{(1)}$ and $\bar{\xi}_s$ counterterms and a single scalar loop remove the overlapping and nested divergences (which are indistinguishable in a theory with scalars only). The remaining $\bar{\alpha}_n^{(2)}$ counterterms are defined to remove the overall divergences, leaving a finite result. These procedures are discussed in Refs. 25 and 28, where the finite, two-loop effective potential is written analytically.

It is important to reiterate several features of the loop expansion, so that they are not obscured by the lengthy manipulations presented above. The Legendre transformation of the connected generating functional produces an effective action that contains only 1-PI contributions. When the effective action is minimized with respect to ϕ , we generate reducible contributions to the energy that contain the coupling constants to all orders. The loop expansion is thus inherently nonperturbative, and the resulting mean field $\bar{\phi}$ also involves all orders in \hbar .

Nevertheless, only the mean field and its effects on the one-body propagator are evaluated nonperturbatively at each order in loops. The loop expansion places primary importance on the mean field. All correlations, both long-range and short-range, are included perturbatively. It is therefore unlike the expansion schemes used in traditional nuclear physics, and it is of interest to see if it provides a useful procedure in QHD. We now generalize the preceding results to QHD-I.

B. The Walecka model

The Lagrangian density is given by²

$$\begin{aligned} \mathcal{L} = & \bar{\psi} [\gamma_\mu (i\partial^\mu - g_v V^\mu) - (M - g_s \phi)] \psi \\ & + \frac{1}{2} (\partial_\mu \phi \partial^\mu \phi - m_s^2 \phi^2) - \frac{1}{4} F_{\mu\nu} F^{\mu\nu} \\ & + \frac{1}{2} m_v^2 V_\mu V^\mu - V(\phi) + \delta\mathcal{L} , \end{aligned} \quad (2.42)$$

where $F^{\mu\nu} = \partial^\mu V^\nu - \partial^\nu V^\mu$. For generality, we will retain the scalar self-interactions, but we are most interested in $V(\phi) = 0$, as in the Lagrangian originally proposed by Walecka.¹ As before, the counterterm piece $\delta\mathcal{L}$ will be specified when necessary.

We will not introduce a chemical potential for the fermions, but rather work in the canonical ensemble at zero temperature and finite baryon density. This will be implemented in the standard fashion through the analytic structure of the baryon propagator.² Since this propagator is modified only by constant mean fields in the loop expansion for infinite matter, the pole structure (see Fig. 32 of Ref. 2) remains the same as in the noninteracting, finite-density propagator. This approach could be generalized by considering the zero-temperature result as the limit of a finite-temperature calculation in Euclidean space; we would then naturally work in the grand canonical ensemble using a chemical potential.^{1,45} This type of treatment will be considered in a covariant framework in a future publication,⁴⁶ but will not be needed in the present work.

The generating functionals for this model are defined as in Eq. (2.4),

$$\begin{aligned} Z[j, J^\mu] & \equiv \exp(iW[j, J^\mu]/\hbar) \\ & \equiv \mathcal{N} \int D(\bar{\psi}) D(\psi) D(\phi) D(V^\mu) \\ & \quad \times \exp \left[\frac{i}{\hbar} \int d^4x [\mathcal{L}(x) + j(x)\phi(x) \right. \\ & \quad \left. + J_\mu(x)V^\mu(x)] \right] , \end{aligned} \quad (2.43)$$

$$\mathcal{N}^{-1} \equiv \int D(\bar{\psi}) D(\psi) D(\phi) D(V^\mu) \exp \left[\frac{i}{\hbar} \int d^4x \mathcal{L}(x) \right] . \quad (2.44)$$

Here the numerator is evaluated in the presence of sources *and at finite density*, as specified by the baryon propagator. In contrast, the normalization factor \mathcal{N} has no sources and is calculated using zero-density baryon propagators, so that it will supply the vacuum subtraction. The squares of the meson masses are shifted by negative imaginary infinitesimals to define the path integrals. It can be shown⁴⁶ that when properly expressed in terms of the dynamical fields \mathbf{V} and their conjugate momenta \mathbf{E} (the electric fields), the vector meson path integral can be rewritten in terms of the four fields V^μ .

The relations between the functionals $W[j, J^\mu]$ and $\Gamma[\phi_e, V_e^\mu]$ and the fields ϕ_e and V_e^μ are analogous to Eqs. (2.6)–(2.11), except that we now have one set of relations

for scalars and one for vectors. In particular, the Legendre transformation (2.8) becomes

$$\begin{aligned} \Gamma[\phi_e, V_e^\mu] & \equiv W[j, J^\mu] \\ & - \int d^4x [j(x)\phi_e(x) + J_\mu(x)V_e^\mu(x)] . \end{aligned} \quad (2.45)$$

In what follows, we work in the rest frame of the nuclear matter and assume that the classical vector fields are purely timelike; for example,

$$V_e^\mu = \delta^{\mu 0} V_e^0 . \quad (2.46)$$

Since the baryon number B and baryon density ρ_B are conserved (we work at fixed volume Ω and let $\Omega \rightarrow \infty$ at the end of the calculation), the mean value of the vector field \bar{V}^0 , obtained by extremizing $\Gamma[\phi_e, V_e^\mu]$ with respect to V_e^0 , is given by the tree-level result *at all orders in loops*:

$$\begin{aligned} \bar{V}^0 & = \hbar \frac{g_v}{m_v^2} \rho_B \\ & \equiv \hbar \frac{g_v}{m_v^2} \frac{\gamma}{(2\pi)^3} \int d^3k \theta(k_F - |\mathbf{k}|) \\ & = \hbar \frac{g_v}{m_v^2} \frac{\gamma k_F^3}{6\pi^2} . \end{aligned} \quad (2.47)$$

(Here k_F is the Fermi momentum and γ is the spin-isospin degeneracy.) We will verify this result explicitly below. It is thus convenient to express the extremized effective action in terms of the mean scalar field $\bar{\phi}$ and baryon density ρ_B , and in analogy to Eq. (2.15), we write the result for uniform fields in terms of the energy density \mathcal{E} :

$$\Gamma[\bar{\phi}, \rho_B] = - \int d^4x \mathcal{E}(\bar{\phi}, \rho_B) . \quad (2.48)$$

At zero baryon density, \mathcal{E} reduces to the scalar effective potential U_{eff} .

The loop expansion in QHD-I now proceeds as in the self-interacting scalar field theory discussed above. One begins by defining classical meson fields that make the action in Eq. (2.43) stationary. This produces Eq. (2.16) for the scalar field and a similar result for the vector field. Since the fermion contributions to Eq. (2.43) involve an extra power of \hbar [see Eq. (2.42)], they do not enter at the classical level. This is not surprising and simply says that one must evaluate loop integrals over fermion propagators to include the effects of these particles. It is possible to restructure the loop expansion so that contributions from “valence” nucleons in the Fermi sea enter at the classical level,^{2,29} but this leads to complicated bookkeeping for the fermions as one proceeds to higher loops.

We will therefore not adopt this procedure, and take the classical field equations to be (2.16) and

$$\begin{aligned} \left[\frac{\delta S[\phi, V^\mu]}{\delta V_\nu(x)} \right]_{V^\mu = V_0^\mu} & = \partial_\mu F_0^{\mu\nu}(x) + m_v^2 V_0^\nu(x) \\ & = -J^\nu(x) . \end{aligned} \quad (2.49)$$

We now expand the generating functional of Eq. (2.43) about the classical fields using Eq. (2.17) and

$$V^\mu(x) \equiv V_0^\mu(x) + \hbar^{1/2} \eta^\mu(x). \quad (2.50)$$

As usual, linear terms in the classical fields vanish by virtue of their field equations, and if we specialize to the renormalizable self-interactions of Eq. (2.26), the connected generating functional can be written as

$$\begin{aligned} \exp \left[\frac{i}{\hbar} W[j, J^\mu] \right] &= \mathcal{N} \exp \left[\frac{i}{\hbar} \left[S[\phi_0, V_0^\mu] + \int d^4x [j(x)\phi_0(x) + J_\mu(x)V_0^\mu(x)] \right] \right] \\ &\times \int D(\bar{\psi})D(\psi)D(\sigma)D(\eta^\mu) \\ &\times \exp \left[i \int d^4x \bar{\psi} [\gamma_\mu (i\partial^\mu - g_v V_0^\mu) - (M - g_s \phi_0)] \psi + \frac{1}{2} \sigma [-\partial^2 - m_s^2 - V''(\phi_0)] \sigma \right. \\ &\quad - \frac{1}{4} (\partial_\mu \eta_\nu - \partial_\nu \eta_\mu)^2 + \frac{1}{2} m_v^2 \eta_\mu \eta^\mu - \hbar^{1/2} g_v \bar{\psi} \gamma_\mu \psi \eta^\mu + \hbar^{1/2} g_s \bar{\psi} \psi \sigma \\ &\quad \left. - \frac{1}{3!} \hbar^{1/2} (\kappa + \lambda \phi_0) \sigma^3 - \frac{1}{4!} \hbar \lambda \sigma^4 \right]. \end{aligned} \quad (2.51)$$

The normalization constant \mathcal{N} has the same form as in Eq. (2.44), except we rescale the boson fields ($\phi \rightarrow \hbar^{1/2} \phi$, $V^\mu \rightarrow \hbar^{1/2} V^\mu$) and cancel the factor of \hbar .

Several comments must be made regarding this result. First, the external sources $j(x)$ and $J_\mu(x)$ couple only to the classical fields. Second, all terms of $O(\hbar^0)$ in the path integral involve Gaussian functional integrals whose results are well known.² The integrals can be performed after we introduce auxiliary sources coupled to σ , η^μ , ψ , and $\bar{\psi}$ [see Eq. (2.20)] and remove the interaction terms. These integrals generate the one-loop terms in the connected generating functional; note that the scalar and baryon propagators are modified, but the vector propagator is not. Finally, the remaining interactions of $O(\hbar^{1/2})$ and higher generate corrections to the one-loop results. These can be computed systematically in powers of \hbar by evaluating the functional derivatives with respect to the auxiliary sources and then setting the sources to zero.

If we carry out the integrals over the quadratic boson terms, we find Eq. (2.22) for the scalars and

$$\bar{I}_0(0) \exp \left[-\frac{i}{2} \int d^4x d^4y U^\mu(x) D_{\mu\nu}^0(x-y) U^\nu(y) \right] \quad (2.52)$$

for the vectors, where U^μ is an auxiliary source,

$$\begin{aligned} D_{\mu\nu}^0(x-y) &= \int \frac{d^4k}{(2\pi)^4} e^{-ik(x-y)} \\ &\times \left[\frac{-g_{\mu\nu} + k_\mu k_\nu / m_v^2}{k^2 - m_v^2 + i\eta} \right], \end{aligned} \quad (2.53)$$

and the constants contained in $\bar{I}_0(0)$ will be absorbed in a new normalization factor \mathcal{N}' , as in Eq. (2.25).

For the baryons, the ‘‘Hartree’’ propagator that arises is given by²

$$\begin{aligned} G^H(x-y) &= \int \frac{d^4p}{(2\pi)^4} \frac{e^{-ip(x-y)}}{\gamma_\mu (p^\mu - g_v V_0^\mu) - (M - g_s \phi_0)} \\ &= e^{-ig_v V_0^\mu(x-y)} \int \frac{d^4t}{(2\pi)^4} \frac{e^{-it(x-y)}}{\gamma_\mu t^\mu - (M - g_s \phi_0)}. \end{aligned} \quad (2.54)$$

Here we have assumed constant classical fields ϕ_0 and V_0^μ . These fields will later be replaced by the mean fields $\bar{\phi}$ and \bar{V}^0 when we perform the loop expansion and extremize the effective action. The boundary conditions on $G^H(x-y)$ are left unspecified in (2.54) and will be imposed by adding suitable imaginary parts to M to generate the analytic structure appropriate for finite density. In practice, this means that the momentum-space propagator separates into two pieces, $G^H(k) \equiv G_F^H(k) + G_D^H(k)$, where G_F^H has a pole structure similar to the Feynman propagator, and G_D^H involves only on-shell propagation in the Fermi sea and is explicitly density dependent.

Note that V_0^μ enters $G^H(x-y)$ *only in the phase*. Since baryon number is conserved, all internal baryon vertices in any Feynman diagram must have one incoming and one outgoing fermion propagator. Thus the factors of V_0^μ will cancel in the evaluation of closed-loop diagrams, such as the effective action and energy density. The only exception to this occurs in the one-loop term, since this depends on the *inverse* of the propagator, as we illustrate shortly. This implies that extremization of the one-loop effective action determines the mean vector field [see Eq. (2.47)], and higher-loop corrections have no effect on this result.

To verify the one-loop contribution, we calculate the fermion path integral²

$$\begin{aligned}
\mathcal{J}_{\phi_0, \nu_0^\mu}[\xi, \bar{\xi}] &\equiv \int D(\bar{\psi})D(\psi) \exp \left[i \int d^4x \{ \bar{\psi} [\gamma_\mu (i\partial^\mu - g_\nu V_0^\mu) - (M - g_s \phi_0)] \psi + \bar{\xi} \psi + \bar{\psi} \xi \} \right] \\
&= \mathcal{J}_0[0,0] \exp \left[\text{Tr} \ln \int d^4z G^0(x-z) [G^H(z-y)]^{-1} \right] \\
&\quad \times \exp \left[-i \int d^4x d^4y \bar{\xi}(x) G^H(x-y) \xi(y) \right], \tag{2.55}
\end{aligned}$$

where ξ and $\bar{\xi}$ are anticommuting (Grassmann) sources. With straightforward manipulations, the initial factor can be rewritten as²

$$\mathcal{J}_0[0,0] \exp \left[\text{Tr} \ln \int d^4z G^0(x-z) [G^H(z-y)]^{-1} \right] = \mathcal{J}_0[0,0] \exp \left[\int d^4x \int \frac{d^4p}{(2\pi)^4} \text{tr} \ln \left[1 + \frac{g_s \phi_0 - g_\nu \gamma_\mu V_0^\mu}{\gamma_\mu p^\mu - M} \right] \right]. \tag{2.56}$$

Here tr denotes a trace over spin and isospin, while Tr also includes a trace over space-time coordinates. The constant $\mathcal{J}_0[0,0]$ will be absorbed in the new normalization \mathcal{N}' , as in Eq. (2.25). Notice that the vector field does not vanish here, which is crucial for producing the correct one-loop results. We have again suppressed the boundary conditions that define the propagator inside the trace, but we will soon see that these can be specified unambiguously at finite density.

With these results, which are valid for constant meson fields, we can write an exact expression for the connected generating functional in the Walecka model as

$$\begin{aligned}
\exp \left[\frac{i}{\hbar} W[j, J^\mu] \right] &= \mathcal{N}' \exp \left[\frac{i}{\hbar} \int d^4x \left(\frac{1}{2} m_\nu^2 V_0^\mu V_{0\mu} - \frac{1}{2} m_s^2 \phi_0^2 + j \phi_0 + J_\mu V_0^\mu \right) \right] \\
&\quad \times \exp \left\{ \int d^4x \left[\int \frac{d^4p}{(2\pi)^4} \text{tr} \ln \left[1 + \frac{g_s \phi_0 - g_\nu \gamma_\mu V_0^\mu}{\gamma_\mu p^\mu - M} \right] + i \sum_{n=1}^4 \frac{1}{n!} \alpha_n^{(1)} \phi_0^n \right] \right\} \\
&\quad \times \left\{ \exp \left[i \int d^4z \left[\sum_{n=1}^4 \hbar^{n/2} a_n^{(1)} \left[\frac{-i\delta}{\delta u} \right]^n + \hbar^{1/2} g_s \left[\frac{i\delta}{\delta \xi} \right] \left[\frac{-i\delta}{\delta \bar{\xi}} \right] \left[\frac{-i\delta}{\delta u} \right] \right. \right. \right. \\
&\quad \left. \left. \left. - \hbar^{1/2} g_\nu \left[\frac{i\delta}{\delta \xi} \right] \gamma_\mu \left[\frac{-i\delta}{\delta \bar{\xi}} \right] \left[\frac{-i\delta}{\delta U_\mu} \right] \right] \right] \right\} \\
&\quad \times \exp \left\{ -\frac{i}{2} \int d^4x d^4y [u(x) \Delta^0(x-y) u(y) + U^\mu(x) D_{\mu\nu}^0(x-y) U^\nu(y)] \right. \\
&\quad \left. - i \int d^4x d^4y \bar{\xi}(x) G^H(x-y) \xi(y) \right\} \Bigg|_{\text{sources}=0}. \tag{2.57}
\end{aligned}$$

Here we have introduced auxiliary sources and $\mathcal{O}(\hbar)$ counterterms $\alpha_n^{(1)}$ [see Eq. (2.29)] that will renormalize fermion loops; the linear combinations $a_n^{(1)}$ are defined as in Eq. (2.31). All the functional derivatives act from the left. Note that in this model, higher-order corrections to the one-loop terms involve the *noninteracting* meson propagators Δ^0 and $D_{\mu\nu}^0$. Equation (2.57) can be easily generalized to include scalar self-interactions by including the vertices, counterterms, and one-loop contributions contained in Eq. (2.32). The scalar propagator Δ^0 must also be replaced by Δ [Eq. (2.23)].

The one-loop contributions to the generating functional are given by the first two exponentials in Eq. (2.57). ($\mathcal{N}'=1$ to this order.) As in the scalar theory, the Legendre transformation is trivial at this level, so we can immediately write the one-loop effective action as

$$\begin{aligned}
\Gamma^{(1)}[\phi_e, V_e^\mu] &= \int d^4x \left[\frac{1}{2} m_\nu^2 V_e^\mu V_{e\mu} - \frac{1}{2} m_s^2 \phi_e^2 \right. \\
&\quad \left. - i \hbar \int \frac{d^4p}{(2\pi)^4} \text{tr} \ln \left[1 + \frac{g_s \phi_e - g_\nu \gamma_\mu V_e^\mu}{\gamma_\mu p^\mu - M} \right] + \hbar \sum_{n=1}^4 \frac{1}{n!} \alpha_n^{(1)} \phi_e^n \right]. \tag{2.58}
\end{aligned}$$

The loop integral over p can be manipulated as described in Ref. 2. We will reproduce those results here in a different fashion to show how to treat the pole structure in the baryon propagator and to illustrate how the renormalization can be carried out without explicitly evaluating the counterterms, which will be useful later. We begin with the identity

$$-i \hbar \int \frac{d^4p}{(2\pi)^4} \text{tr} \ln \left[1 + \frac{g_s \phi_e - g_\nu \gamma_\mu V_e^\mu}{\gamma_\mu p^\mu - M} \right] = i \hbar \int \frac{d^4p}{(2\pi)^4} \text{tr} \left[\gamma_0 p^0 \left[\frac{1}{\gamma_\mu p^\mu - g_\nu \gamma_\mu V_e^\mu - (M - g_s \phi_e)} - \frac{1}{\gamma_\mu p^\mu - M} \right] \right]. \tag{2.59}$$

This relation was derived in Ref. 2 for a classical scalar field, and with proper care regarding the ordering of factors, it can be extended to include a classical vector field. The integrals have been regularized by writing them in τ dimensions;

physical results are obtained by taking $\tau \rightarrow 4^-$ after the renormalization has been performed.⁴⁷

We can now impose boundary conditions on the propagators in Eq. (2.59). For the term involving the (constant) meson fields, we work at finite density by writing

$$G^H(p) \equiv \frac{1}{\gamma_\mu p^\mu - g_v \gamma_\mu V_e^\mu - (M - g_s \phi_e)} \\ \equiv (\gamma_\mu p^\mu - g_v \gamma_\mu V_e^\mu + M - g_s \phi_e) \left[\frac{1}{(p - g_v V_e)^2 - (M - g_s \phi_e)^2 + i\eta} + \frac{i\pi}{E^*(p)} \delta[p^0 - E(p)] \theta(k_F - |\mathbf{p}|) \right] \quad (2.60)$$

$$\equiv G_F^H(p) + G_D^H(p), \quad (2.61)$$

where $E^*(p) \equiv [p^2 + (M - g_s \phi_e)^2]^{1/2}$ and $E(p) \equiv g_v V_e^0 + E^*(p)$. $G_D^H(p)$ arises from shifting the poles from the fourth to the first quadrant of the p^0 plane for occupied states inside the Fermi sea. The second propagator in (2.59) is evaluated in the vacuum in the absence of meson fields and therefore carries the usual Feynman prescription for the pole: $M \rightarrow M - i\eta$.

These expressions can be inserted into Eq. (2.58) and the integrals over the Fermi sea performed, producing

$$\Gamma^{(1)}[\phi_e, V_e^0] = \int d^4x \left[\frac{1}{2} m_v^2 (V_e^0)^2 - \frac{1}{2} m_s^2 \phi_e^2 - \hbar g_v V_e^0 \rho_B - \hbar \frac{\gamma}{(2\pi)^3} \int d^3p E^*(p) \theta(k_F - |\mathbf{p}|) \right. \\ \left. + i\hbar \int \frac{d^4p}{(2\pi)^4} \{ \text{tr}[\gamma^0 G_F^*(p)] - \text{tr}[\gamma^0 G_F^0(p)] \} p^0 + \hbar \sum_{n=1}^4 \frac{1}{n!} \alpha_n^{(1)} \phi_e^n \right], \quad (2.62)$$

where G_F^0 is the Feynman propagator in the vacuum. The dimensional regularization has allowed us to shift variables in the first integral, *eliminating the dependence on the vector field*,⁴⁸ so that it can be expressed in terms of the simpler propagator

$$G^*(p) \equiv (\gamma_\mu p^\mu + M^*) \\ \times \left[\frac{1}{p^2 - M^{*2} + i\eta} + \frac{i\pi}{E^*(p)} \delta[p^0 - E^*(p)] \theta(k_F - |\mathbf{p}|) \right] \quad (2.63)$$

$$\equiv G_F^*(p) + G_D^*(p), \quad (2.64)$$

where $M^* \equiv M - g_s \phi_e$. Since the uniform vector field has vanished from the divergent one-loop corrections, no vector counterterms are required.

To remove the divergences and define the $O(\hbar)$ counterterms, we use the algebraic identity ("Furry expansion")

$$G_F^*(k) = \sum_{i=0}^m (M^* - M)^i [G_F^0(k)]^{i+1} \\ + (M^* - M)^{m+1} [G_F^0(k)]^{m+1} G_F^*(k), \quad (2.65)$$

which is valid for any m , and the Ward identity

$$-\frac{\partial}{\partial k^0} G_F^0(k) = G_F^0(k) \gamma^0 G_F^0(k). \quad (2.66)$$

One can then insert Eq. (2.65) with $m=4$ into Eq. (2.62). The term independent of ϕ_e is removed by the vacuum subtraction contained in the integral over G_F^0 . The next four terms in the expansion are divergent but can be removed by defining the counterterms

$$\alpha_n^{(1)} \equiv i(-1)^{n+1} g_s^n \int \frac{d^4k}{(2\pi)^4} \text{tr} \left[\frac{\partial^{n-1}}{\partial M^{n-1}} G_F^0(k) \right]. \quad (2.67)$$

These agree with the one-loop counterterms obtained by renormalizing the scalar propagator and vertices at zero external momenta (see Fig. 35 of Ref. 2). Note that Eq. (2.66) and $\partial G_F^0(k)/\partial M = [G_F^0(k)]^2$ were used to arrive at (2.67). The remaining term in the expansion is at least $O(\phi_e^5)$ and is explicitly finite by power counting; thus the limit $\tau \rightarrow 4^-$ can be taken.

The finite one-loop effective action thus becomes

$$\Gamma^{(1)}[\phi_e, V_e^0] = \int d^4x \left[\frac{1}{2} m_v^2 (V_e^0)^2 - \frac{1}{2} m_s^2 \phi_e^2 - \hbar g_v V_e^0 \rho_B - \hbar \frac{\gamma}{(2\pi)^3} \int d^3p E^*(p) \theta(k_F - |\mathbf{p}|) - \Delta \mathcal{E}(M^*) \right], \quad (2.68)$$

where

$$\Delta \mathcal{E}(M^*) \equiv -i\hbar (M^* - M)^5 \int \frac{d^4k}{(2\pi)^4} \text{tr} \{ \gamma^0 [G_F^0(k)]^5 G_F^*(k) \} k^0 \quad (2.69)$$

$$= -\tilde{\hbar} \frac{\gamma}{16\pi^2} [M^{*4} \ln(M^*/M) + M^3(M - M^*) - \frac{7}{2} M^2(M - M^*)^2 + \frac{13}{3} M(M - M^*)^3 - \frac{25}{12} (M - M^*)^4], \quad (2.70)$$

which has no explicit dependence on k_F . Henceforth, we assume that the spin-isospin degeneracy of the vacuum is $\gamma=4$. Notice that we have obtained a finite $\Delta\mathcal{E}$ without evaluating divergent integrals or counterterms explicitly. Nevertheless, this finite result depends on the choice of renormalization conditions, which contain some arbitrariness. By renormalizing at zero external momenta for the scalar propagator and vertices, the effective action takes a simple form. However, the usual “on-shell” conditions for these scalar n -point functions are now violated by the one-loop corrections. This is not a problem, since there are no experimental sources of free scalar mesons, but in principle, one could renormalize at $p^2=m_s^2$, or indeed, any other mass scale. In addition, the ϕ^3 and ϕ^4 counterterms are defined to remove such terms from the effective potential, in accord with Walecka’s original definition of the Lagrangian (2.42). This implies that the renormalized cubic and quartic scalar couplings vanish at vanishing scalar-meson momenta. One is free to include these terms in the effective potential if desired by altering the finite parts of the counterterms. We emphasize, however, that in a renormalizable theory, $\mathcal{O}(\phi_e^5)$ and higher terms cannot be removed from $\Delta\mathcal{E}$.

To determine the one-loop energy density [see Eq. (2.48)], the effective action must be extremized with respect to ϕ_e and V_e^0 . Since the factors of V_e^0 are explicit, the extremization produces Eq. (2.47), as advertised. The minimization with respect to ϕ_e produces the familiar one-loop [or relativistic Hartree approximation (RHA)] self-consistency condition

$$M^* = M - \frac{g_s^2}{m_s^2} \frac{\gamma}{(2\pi)^3} \int_0^{k_F} d^3p \frac{M^*}{E^*(p)} + \frac{g_s^2}{m_s^2} \frac{1}{\pi^2} [M^{*3} \ln(M^*/M) - M^2(M^* - M) - \frac{5}{2} M(M^* - M)^2 - \frac{11}{6} (M^* - M)^3]. \quad (2.71)$$

Notice that the solution to this equation involves all orders in g_s^2 . Since all terms in Eq. (2.68) are independent of space-time, the one-loop energy density is given by

$$\mathcal{E}^{(1)}(M^*, \rho_B) = \frac{g_v^2}{2m_v^2} \rho_B^2 + \frac{m_s^2}{2g_s^2} (M - M^*)^2 + \frac{\gamma}{(2\pi)^3} \int_0^{k_F} d^3p E^*(p) + \Delta\mathcal{E}(M^*), \quad (2.72)$$

where we have suppressed factors of $\tilde{\hbar}$, and M^* is determined at each ρ_B by solving Eq. (2.71). We remark that although $\Delta\mathcal{E}$ has historically been called the “vacuum fluctuation correction,” this appellation is unfortunate, since it does not involve any fluctuations. More precisely, $\Delta\mathcal{E}$ is the finite shift in the baryon zero-point energy that occurs at finite density.

To compute the two-loop corrections, we follow our previous analysis of the interacting scalar field theory. The contributions to the connected generating functional \mathcal{W} can be determined by retaining the $\mathcal{O}(\tilde{\hbar})$ functional derivatives in Eq. (2.57). Notice that each coupling constant is accompanied by a power of $\tilde{\hbar}^{1/2}$, so that the loop expansion is perturbative in the couplings, but nonperturbative in the mean fields, as it involves the Hartree propagator G^H . There are also vacuum subtractions arising from \mathcal{N} that are computed from a similar expression with $\phi_0 = V_0^\mu = 0$; we will exhibit these explicitly below.

The two-loop effective action takes a form analogous to Eq. (2.34), and the analysis leading to Eq. (2.37) goes through as before, except that there are now scalar and vector pieces, and we drop the scalar self-interactions. We find

$$\Gamma^{(2)}[\phi_e, V_e^0] = \Gamma^{(1)}[\phi_e, V_e^0] + W_2[\phi_e] + \frac{1}{2} \int d^4x d^4y \left[\frac{\delta W_1}{\delta \phi_0(x)} \right] \Delta^0(x-y) \left[\frac{\delta W_1}{\delta \phi_0(y)} \right] - \frac{1}{2} \delta^{\mu 0} \delta^{\nu 0} \int d^4x d^4y \left[\frac{\delta W_1}{\delta V_0^\mu(x)} \right] D^0(x-y) \left[\frac{\delta W_1}{\delta V_0^\nu(y)} \right] + \mathcal{O}(\tilde{\hbar}^3), \quad (2.73)$$

where the double integrals are evaluated with

$$\left[\frac{\delta W_1[\phi_0, V_0^\mu]}{\delta \phi_0} \right]_{\phi_0 = \phi_e} = -i\tilde{\hbar}g_s \int \frac{d^4p}{(2\pi)^4} \text{tr} G^H(p) + \tilde{\hbar}a_1^{(1)}(\phi_e), \quad (2.74)$$

$$\left[\frac{\delta W_1[\phi_0, V_0^\mu]}{\delta V_0^\nu} \right]_{V_0^\mu = \delta^{\mu 0} V_e^0} = i\tilde{\hbar}g_v \delta_{\nu 0} \int \frac{d^4p}{(2\pi)^4} \text{tr} \gamma^0 G^H(p), \quad (2.75)$$

using $G^H(p)$ from Eq. (2.60) and $a_1^{(1)}(\phi)$ defined as in (2.31). Here

$$D^0(x-y) \equiv \int \frac{d^4k}{(2\pi)^4} \frac{e^{-ik(x-y)}}{k^2 - m_v^2 + i\eta} \equiv \int \frac{d^4k}{(2\pi)^4} e^{-ik(x-y)} D^0(k), \quad (2.76)$$

since the longitudinal ($k_\mu k_\nu$) term in the propagator (2.53) does not contribute by the conservation of the baryon current, and spatial components of V_e^μ vanish in the nuclear matter rest frame. Note also that W_2 is independent of V_e^0 , since this field enters only in the phase of the Hartree propagator and vanishes for closed loops, as discussed above.

Since the fields are assumed constant and uniform, it again follows that the double integrals in (2.73) produce one-particle reducible contributions that cancel those arising in $W_2[\phi_e]$, leaving only irreducible terms in $\Gamma^{(2)}$. There are four types of counterterm subtractions that enter in order \hbar^2 . First, there are the $O(\hbar)$ counterterms $a_n^{(1)}$ contained in (2.57) that multiply a single scalar loop. Second, we must add $O(\hbar^2)$ counterterms $\alpha_n^{(2)}$ of the same form as Eq. (2.29). Third, there are scalar and vector wave-function counterterms arising from

$$\delta\mathcal{L}' = \frac{\hbar}{2}\zeta_s\partial^\mu\phi\partial_\mu\phi - \frac{\hbar}{4}\zeta_v(\partial_\mu V_\nu - \partial_\nu V_\mu)^2 = -\frac{\hbar^2}{2}\zeta_s\sigma\partial^2\sigma - \frac{\hbar^2}{2}\zeta_v(\partial_\mu\eta_\nu - \partial_\nu\eta_\mu)\partial^\mu\eta^\nu. \quad (2.77)$$

Although these contributions are ostensibly of $O(\hbar)$, the leading terms vanish because the mean fields are uniform. Finally, there are counterterms for the baryon mass and wave function and also the baryon-scalar vertex. These take the form

$$\delta\mathcal{L}'' = \hbar^2[M_c\bar{\psi}\psi - \zeta_N\bar{\psi}(i\gamma_\mu\partial^\mu - M)\psi + \gamma_s\bar{\psi}\psi\phi] \quad (2.78)$$

and enter first at two-loop order since they multiply bilinear terms in the baryon fields. They will appear in the two-loop effective action as constants multiplying a single baryon loop. Since the two-loop corrections are independent of the vector field, no counterterm is needed for the baryon-vector vertex when we renormalize at zero external momentum.

After inserting the new counterterms into Eq. (2.57), it is straightforward to expand this expression to the desired order and compute $W_2[\phi_0]$. As before, the Legendre transformation of this piece is obtained by simply replacing ϕ_0 with ϕ_e . Since the fields are constant and uniform, the $\int d^4x$ is an (infinite) multiplicative factor that disappears in the definition of the two-loop energy density. We obtain

$$\begin{aligned} \mathcal{E}^{(2)}(M^*, \rho_B) &= \mathcal{E}^{(1)}(M^*, \rho_B) + \frac{1}{2}g_s^2 \int \frac{d^\tau k}{(2\pi)^4} \frac{d^\tau q}{(2\pi)^4} \text{tr}[G^*(k)G^*(q)]\Delta^0(k-q) \\ &\quad - \frac{1}{2}g_v^2 \int \frac{d^\tau k}{(2\pi)^4} \frac{d^\tau q}{(2\pi)^4} \text{tr}[\gamma_\mu G^*(k)\gamma^\mu G^*(q)]D^0(k-q) - \frac{i}{2}(\alpha_2^{(1)} + \alpha_3^{(1)}\phi + \frac{1}{2}\alpha_4^{(1)}\phi^2) \int \frac{d^\tau k}{(2\pi)^4} \Delta^0(k) \\ &\quad - \frac{i}{2}\zeta_s \int \frac{d^\tau k}{(2\pi)^4} k^2 \Delta^0(k) - \frac{3i}{2}\zeta_v \int \frac{d^\tau k}{(2\pi)^4} k^2 D^0(k) + i(M_c + \gamma_s\phi) \int \frac{d^\tau k}{(2\pi)^4} \text{tr}[G^*(k)] \\ &\quad - i\zeta_N \int \frac{d^\tau k}{(2\pi)^4} \text{tr}[(\gamma_\mu k^\mu - M)G^*(k)] - \sum_{n=1}^4 \frac{1}{n!} \alpha_n^{(2)} \phi^n - \text{VEV}. \end{aligned} \quad (2.79)$$

Here we have suppressed factors of \hbar and written $M^* = M - g_s\phi$. Note that $G^*(k)$ contains both the Feynman and density-dependent pieces from Eq. (2.64). The correct value of M^* (or ϕ) is determined by extremizing (2.79) with respect to this parameter. Since W_2 is independent of the vector field, the extremization of $\Gamma^{(2)}$ with respect to V_e^0 again yields Eq. (2.47), which has been used to write $\mathcal{E}^{(1)}$.

We remark that Eq. (2.79) is exactly what would be obtained if one used second-order perturbation theory around the one-loop (RHA) ground state [described by Eqs. (2.72) and (2.63)] and kept only the 1-PI pieces. Our expression thus generalizes the results of Chin, who used perturbation theory on the *noninteracting* ground state ($M^* = M$) and obtained only the two-loop terms with explicit density dependence.⁷ In contrast, our expression contains two-loop corrections arising from the dynamical quantum vacuum, which will be discussed shortly.

The VEV subtraction can be deduced from an expression analogous to (2.57) with the classical fields set to zero and G^H replaced by G_F^0 . A straightforward calculation produces

$$\begin{aligned} \text{VEV} &= -\frac{i}{2}\alpha_2^{(1)} \int \frac{d^\tau k}{(2\pi)^4} \Delta^0(k) - \frac{i}{2}\zeta_s \int \frac{d^\tau k}{(2\pi)^4} k^2 \Delta^0(k) - \frac{3i}{2}\zeta_v \int \frac{d^\tau k}{(2\pi)^4} k^2 D^0(k) \\ &\quad + iM_c \int \frac{d^\tau k}{(2\pi)^4} \text{tr}[G_F^0(k)] - i\zeta_N \int \frac{d^\tau k}{(2\pi)^4} \text{tr}[(\gamma_\mu k^\mu - M)G_F^0(k)] \\ &\quad + \frac{1}{2}g_s^2 \int \frac{d^\tau k}{(2\pi)^4} \frac{d^\tau q}{(2\pi)^4} \text{tr}[G_F^0(k)G_F^0(q)]\Delta^0(k-q) - \frac{1}{2}g_v^2 \int \frac{d^\tau k}{(2\pi)^4} \frac{d^\tau q}{(2\pi)^4} \text{tr}[\gamma_\mu G_F^0(k)\gamma^\mu G_F^0(q)]D^0(k-q). \end{aligned} \quad (2.80)$$

Note that the vertex counterterms $\alpha_3^{(1)}$, $\alpha_4^{(1)}$, and γ_s do not enter here because $\phi_0 = 0$ in the vacuum.

The divergent double integrals in Eq. (2.79) have been regularized in τ dimensions. To arrive at finite results, these must be combined with the counterterms and VEV subtraction. As a first step, we rewrite the integrals by splitting the

baryon propagator into Feynman and density-dependent parts, as in Eq. (2.64). Thus, for the scalar contribution, we find

$$\begin{aligned}
& \frac{1}{2}g_s^2 \int \frac{d^\tau k}{(2\pi)^4} \frac{d^\tau q}{(2\pi)^4} \text{tr}[G^*(k)G^*(q)]\Delta^0(k-q) \\
&= \frac{1}{2}g_s^2 \int \frac{d^\tau k}{(2\pi)^4} \frac{d^\tau q}{(2\pi)^4} \text{tr}[G_F^*(k)G_F^*(q)]\Delta^0(k-q) + g_s^2 \int \frac{d^\tau k}{(2\pi)^4} \frac{d^\tau q}{(2\pi)^4} \text{tr}[G_D^*(k)G_F^*(q)]\Delta^0(k-q) \\
&+ \frac{1}{2}g_s^2 \int \frac{d^\tau k}{(2\pi)^4} \frac{d^\tau q}{(2\pi)^4} \text{tr}[G_D^*(k)G_D^*(q)]\Delta^0(k-q) \\
&= \frac{1}{2}g_s^2 \int \frac{d^\tau k}{(2\pi)^4} \frac{d^\tau q}{(2\pi)^4} \text{tr}[G_F^*(k)G_F^*(q)]\Delta^0(k-q) - i \int \frac{d^\tau k}{(2\pi)^4} \text{tr}[G_D^*(k)\Sigma_F^s(k)] - \frac{i}{2} \int \frac{d^4 k}{(2\pi)^4} \text{tr}[G_D^*(k)\Sigma_D^s(k)], \quad (2.81)
\end{aligned}$$

where the scalar parts of the Feynman (Σ_F^s) and density-dependent (Σ_D^s) baryon self-energy are defined in Appendix A. A similar decomposition holds for the integral involving vector-meson exchange, except now factors of γ_μ and γ^μ appear between $G^*(k)$ and $G^*(q)$, and the self-energies are replaced by the vector contributions ($-\gamma_\mu \Sigma_F^{v\mu}$) and ($-\gamma_\mu \Sigma_D^{v\mu}$).

With this decomposition, the energy density through two-loop order can be written as

$$\mathcal{E}^{(2)}(M^*, \rho_B) = \mathcal{E}^{(1)}(M^*, \rho_B) + \mathcal{E}_{\text{ex}}^{(2)}(M^*, \rho_B) + \mathcal{E}_{\text{LS}}^{(2)}(M^*, \rho_B) + \mathcal{E}_{\text{VF}}^{(2)}(M^*), \quad (2.82)$$

and we can discuss each of the two-loop pieces separately. The first piece,

$$\mathcal{E}_{\text{ex}}^{(2)}(M^*, \rho_B) = -\frac{i}{2} \int \frac{d^4 k}{(2\pi)^4} \text{tr}\{G_D^*(k)[\Sigma_D^s(k) - \gamma_\mu \Sigma_D^{v\mu}(k)]\}, \quad (2.83)$$

is finite, since it contains two G_D^* propagators that restrict the integration to the filled Fermi sea. This term generates the exchange of identical fermions in occupied states, just as in nonrelativistic Hartree-Fock calculations, and we call it the ‘‘exchange term.’’ These exchange contributions are precisely those studied by Chin,⁷ and if classified in powers of the coupling constants, they reproduce the lowest-order exchange contributions in the self-consistent Dirac-Hartree-Fock calculations of Refs. 49–53.

The second two-loop term can be written as

$$\begin{aligned}
\mathcal{E}_{\text{LS}}^{(2)}(M^*, \rho_B) &= -i \int \frac{d^4 k}{(2\pi)^4} \text{tr}[\Sigma_F^s(k)G_D^*(k)] + i \int \frac{d^4 k}{(2\pi)^4} \text{tr}[\gamma_\mu \Sigma_F^{v\mu}(k)G_D^*(k)] \\
&+ i(M_c + \gamma_s \phi) \int \frac{d^4 k}{(2\pi)^4} \text{tr}[G_D^*(k)] - i\zeta_N \int \frac{d^4 k}{(2\pi)^4} \text{tr}[(\gamma_\mu k^\mu - M)G_D^*(k)]. \quad (2.84)
\end{aligned}$$

Here the baryon counterterm subtractions proportional to G_D^* [see Eq. (2.79)] have been included, and they renormalize the Feynman self-energy $\Sigma_F \equiv \Sigma_F^s - \gamma_\mu \Sigma_F^{v\mu}$. Since the integrals over k are cut off by $G_D^*(k)$, the only divergences occur in the self-energy, and since $G_D^* \rightarrow 0$ at zero density, no VEV subtraction is needed. $\mathcal{E}_{\text{LS}}^{(2)}$ is analogous to the Lamb shift in atomic physics, since it involves particles in occupied states whose spectrum is shifted by interaction with the fluctuating meson fields at finite density. The counterterm subtractions simply remove the fluctuations that would occur in free space, where $M^* = M$. (Alternatively, one can interpret $\mathcal{E}_{\text{LS}}^{(2)}$ as arising from modifications of the quantum vacuum due to the Pauli blocking of intermediate states at finite density.)

The final two-loop contribution is

$$\begin{aligned}
\mathcal{E}_{\text{VF}}^{(2)}(M^*) &= \frac{1}{2}g_s^2 \int \frac{d^\tau k}{(2\pi)^4} \frac{d^\tau q}{(2\pi)^4} \text{tr}[G_F^*(k)G_F^*(q)]\Delta^0(k-q) \\
&- \frac{1}{2}g_v^2 \int \frac{d^\tau k}{(2\pi)^4} \frac{d^\tau q}{(2\pi)^4} \text{tr}[\gamma_\mu G_F^*(k)\gamma^\mu G_F^*(q)]D^0(k-q) - \frac{i}{2}(\alpha_2^{(1)} + \alpha_3^{(1)}\phi + \frac{1}{2}\alpha_4^{(1)}\phi^2) \int \frac{d^\tau k}{(2\pi)^4} \Delta^0(k) \\
&- \frac{i}{2}\zeta_s \int \frac{d^\tau k}{(2\pi)^4} k^2 \Delta^0(k) - \frac{3i}{2}\zeta_v \int \frac{d^\tau k}{(2\pi)^4} k^2 D^0(k) + i(M_c + \gamma_s \phi) \int \frac{d^\tau k}{(2\pi)^4} \text{tr}[G_F^*(k)] \\
&- i\zeta_N \int \frac{d^\tau k}{(2\pi)^4} \text{tr}[(\gamma_\mu k^\mu - M)G_F^*(k)] - \sum_{n=1}^4 \frac{1}{n!} \alpha_n^{(2)} \phi^n - \text{VEV}, \quad (2.85)
\end{aligned}$$

where the VEV subtraction is given by Eq. (2.80). $\mathcal{E}_{\text{VF}}^{(2)}$ is a true vacuum fluctuation correction, since it involves virtual excitation of both mesons and baryons. The integrals contain nested, overlapping, and overall divergences, which are defined below, and we will return shortly to discuss the renormalization procedure.

First, however, we derive expressions for $\mathcal{E}_{\text{ex}}^{(2)}$ and $\mathcal{E}_{\text{LS}}^{(2)}$ that can be used for numerical computation. With Eqs. (2.63), (A3), and (A4), the calculation of the finite $\mathcal{E}_{\text{ex}}^{(2)}$ is straightforward, leading to

$$\begin{aligned} \mathcal{E}_{\text{ex}}^{(2)}(M^*, \rho_B) = & \gamma g_s^2 \int \frac{d^3 q}{(2\pi)^3} \frac{d^3 k}{(2\pi)^3} \frac{n_q^0}{2E^*(q)} \frac{n_k^0}{2E^*(k)} \left[\frac{E^*(k)E^*(q) + M^{*2} - \mathbf{k} \cdot \mathbf{q}}{(\mathbf{k} - \mathbf{q})^2 - [E^*(k) - E^*(q)]^2 + m_s^2} \right] \\ & + 2\gamma g_v^2 \int \frac{d^3 q}{(2\pi)^3} \frac{d^3 k}{(2\pi)^3} \frac{n_q^0}{2E^*(q)} \frac{n_k^0}{2E^*(k)} \left[\frac{E^*(k)E^*(q) - 2M^{*2} - \mathbf{k} \cdot \mathbf{q}}{(\mathbf{k} - \mathbf{q})^2 - [E^*(k) - E^*(q)]^2 + m_v^2} \right]. \end{aligned} \quad (2.86)$$

Here γ is the spin-isospin degeneracy, the Fermi distribution functions are written as $n_k^0 \equiv \theta(k_F - |\mathbf{k}|)$, and $E^*(k) \equiv (\mathbf{k}^2 + M^{*2})^{1/2}$. These results agree with those of Chin.⁷ The angular integrals can be done analytically [see Eq. (5.79) in Ref. 2] leaving a compact, two-dimensional integral that can be evaluated accurately with Gaussian quadrature.

To produce a finite result for the Lamb shift $\mathcal{E}_{\text{LS}}^{(2)}$, the divergences contained in $\Sigma_F^s - \gamma_\mu \Sigma_F^{v\mu}$ must be renormalized. To isolate the divergences, write the two-loop integrals in Eq. (2.84) as

$$\int \frac{d^4 k}{(2\pi)^4} \int \frac{d^4 q}{(2\pi)^4} \text{tr} \{ G_D^*(k) [g_s^2 G_F^*(q) \Delta^0(k - q) - g_v^2 \gamma_\mu G_F^*(q) \gamma^\mu D^0(k - q)] \} \quad (2.87)$$

and expand the factors of G_F^* as power series in M^* , using Eq. (2.65).

Power counting reveals that only the first two terms in this expansion diverge, implying that mass, wave-function, and scalar vertex counterterms are needed to render the integrals finite. These counterterms are defined and evaluated in Appendix A. With the relations in that Appendix, it is easy to see that the counterterms in Eq. (2.84) remove the divergences, leading to a result containing renormalized Feynman self-energies,

$$\begin{aligned} \mathcal{E}_{\text{LS}}^{(2)}(M^*, \rho_B) = & -i \int \frac{d^4 k}{(2\pi)^4} \text{tr} \{ [\Sigma_{RF}^s(k) - \gamma_\mu \Sigma_{RF}^{v\mu}(k)] G_D^*(k) \} \\ = & \rho_s(M^*, \rho_B) \left\{ \frac{g_s^2}{16\pi^2} \left[M^* \int_0^1 dx (1+x) \ln \left[\frac{M^{*2}(1-x)^2 + m_s^2 x}{M^2(1-x)^2 + m_s^2 x} \right] \right. \right. \\ & \left. \left. + 2M^2(M - M^*) \int_0^1 dx \frac{(1-x)(1-x^2)}{M^2(1-x)^2 + m_s^2 x} \right] \right. \\ & \left. - \frac{g_v^2}{8\pi^2} \left[M^* \int_0^1 dx (2-x) \ln \left[\frac{M^{*2}(1-x)^2 + m_v^2 x}{M^2(1-x)^2 + m_v^2 x} \right] \right. \right. \\ & \left. \left. + 2M^2(M - M^*) \int_0^1 dx \frac{(1-x)^2(2-x)}{M^2(1-x)^2 + m_v^2 x} \right] \right\}. \end{aligned} \quad (2.88)$$

Here ρ_s is the scalar density of baryons

$$\rho_s(M^*, \rho_B) \equiv \frac{\gamma}{(2\pi)^3} \int d^3 k \frac{M^*}{E^*(k)} n_k^0. \quad (2.89)$$

By expanding the logarithms about $M^* = M$, one can verify that the Lamb shift contribution begins at $O[(M - M^*)^2]$. This is in agreement with Eq. (A13), since the counterterms explicitly remove the constant and linear terms in this expansion. The integrals in Eq. (2.88) can be evaluated analytically, but Gaussian quadrature is accurate to 1 ppm with a modest number of points (≈ 16).

Finally, we consider the vacuum fluctuation contribution $\mathcal{E}_{\text{VF}}^{(2)}$, whose renormalization is the primary difficulty in the two-loop calculation. We will describe the renormalization procedure for the scalar loops, but the vector

terms can be treated analogously, since the integrals are independent of the vector field \vec{V}^0 . An alternative approach to the renormalization is presented in Appendix C.

Let us begin by classifying the divergences contained in the double integrals in Eq. (2.85). This is most easily done using the terminology of 't Hooft and Veltman,⁴⁷ who label the three internal lines α , β , and γ , as shown in Fig. 2. The simplest divergences arise from the subintegrals $\alpha\gamma$ and $\beta\gamma$. These are "nested divergences" that occur when $k \rightarrow \infty$ with q fixed, or vice versa, and they can be removed by renormalizing the subdiagrams for the baryon self-energy and baryon-scalar vertex. It is also obvious that there are overall divergences in the $\alpha\beta\gamma$ integral when both $k \rightarrow \infty$ and $q \rightarrow \infty$. Finally, the trickiest divergences arise from the $\alpha\beta$ loop. These are called

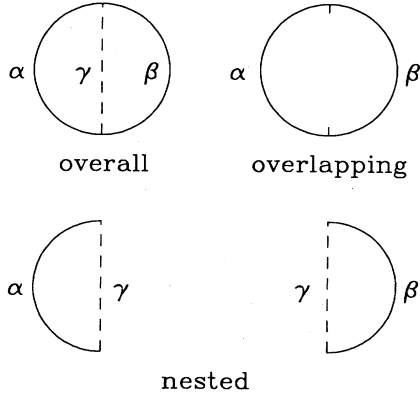


FIG. 2. Classification of divergences in the two-loop contributions to the energy density. The solid line is a baryon propagator and the dashed line is a scalar meson propagator.

overlapping divergences and occur when $(k - q)$ is fixed, but $(k + q)$ becomes large. (These are easiest to see by first changing variables $k \rightarrow k + q$ and then letting $q \rightarrow \infty$.) Since the overlapping divergences arise from the fermion loop, while the momentum in the meson propagator is fixed, they are removed by renormalizing the one-loop scalar propagator and scalar vertices. The integrals in Eq. (2.85) have logarithmic nested divergences, quadratic overlapping divergences, and quartic overall divergences.

To isolate and renormalize these contributions, we expand the fermion propagators G_F^* in powers of $M - M^* = g_s \phi$, as shown in Fig. 3. Here the solid lines represent noninteracting Feynman propagators G_F^0 , the dashed lines are noninteracting meson propagators Δ^0 , crosses signify factors of $(-g_s \phi)$, and the letters denote the type of divergence: n =nested, p =overlapping, and a =overall. Note that all diagrams in the lower right-hand corner (containing at least five powers of ϕ) are finite. The diagrams in the first two rows and first two columns contain nested divergences to *all orders* in ϕ that are removed by the M_c , ξ_N , and γ_s counterterms defined in Appendix A. Notice that these subtractions appear in Eq. (2.85) in conjunction with an integral over G_F^* , which also contains all powers of ϕ . Overlapping divergences occur only in diagrams with two or fewer factors of ϕ , and are removed by the $\alpha_n^{(1)}$ and ξ_s counterterm subtractions. The $\alpha_n^{(1)}$ counterterms are defined in Eq. (2.67), and note that the subtractions include terms only through order ϕ^2 .

We are left with only overall divergences. For the terms proportional to ϕ^n ($1 \leq n \leq 4$), the subtractions are made by defining the $\alpha_n^{(2)}$ counterterms to cancel the relevant loop integrals *with the nested and overlapping divergences removed*. Explicit expressions for these counterterms are given in Appendix B. The final overall divergence (in the upper left-hand corner of Fig. 3) is independent of ϕ and is removed by the vacuum subtraction of Eq. (2.80). The counterterms in Eq. (2.80) eliminate the nested and overlapping divergences from the double integral in that expression, leaving only the

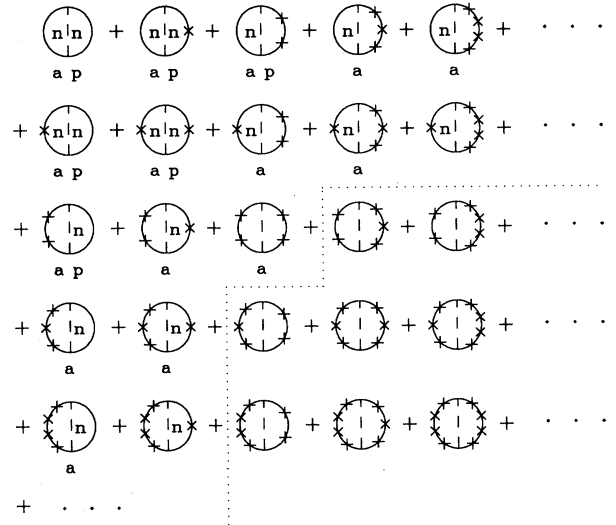


FIG. 3. Expansion of the two-loop vacuum fluctuation correction in powers of the scalar field. The diagrams to the lower right of the dotted line are finite.

overall divergence, which is all that is required for the subtraction.

Since the QHD-I Lagrangian (2.42) is globally gauge invariant, no counterterms of the form $V_\mu V^\mu$, $\phi V_\mu V^\mu$, or $\phi^2 V_\mu V^\mu$ are needed to renormalize the one-loop vector meson propagator⁵⁴ or vector-scalar vertices.⁵⁵ The two-loop integral involving vector mesons has only a single overlapping divergence, which occurs in the contribution that is independent of ϕ and is removed by the vector wave-function counterterm ξ_v . This counterterm appears in the VEV subtraction for the same reason, and evidently, one could omit this counterterm entirely (at this order in \hbar) and still arrive at finite results.

We emphasize two important points. First, the preceding discussion shows that a systematic expansion of the exact generating functional [Eq. (2.57)], including the normalization factor \mathcal{N} , produces all required counterterm subtractions to any order in \hbar . Divergent subintegrals will always be renormalized by lower-order counterterms, which is a realization of the well-known “forest formula” for renormalization.^{6,15,56} Thus the loop expansion can be carried out unambiguously to any order in loops. Second, as in the one-loop calculation, the two-loop counterterms $\alpha_n^{(2)}$ are defined to completely eliminate all terms through order ϕ^4 in the expansion of $\mathcal{E}_{VF}^{(2)}$. This leaves a result that begins at order ϕ^5 and is consistent with Walecka’s original definition of the model, which has no nonlinear scalar couplings. If desired, one could include finite ϕ^3 and ϕ^4 interactions by modifying the $\alpha_3^{(2)}$ and $\alpha_4^{(2)}$ counterterms.

In practice, the simplest way to produce a finite result for $\mathcal{E}_{VF}^{(2)}$ is to use Eq. (2.65) to isolate all contributions through order ϕ^4 , while leaving the remaining integrals in terms of G_F^* . It is then a straightforward matter of algebra (see the discussion at the end of Appendix B) to show that the counterterms defined in Eqs. (2.67), (A10)–(A12), and (B6) remove the divergences, leading to

$$\begin{aligned}
\mathcal{G}_{\text{VF}}^{(2)}(M^*) = & (M^* - M)^5 \left[\frac{1}{2} g_s^2 \int \frac{d^4 k}{(2\pi)^4} \frac{d^4 q}{(2\pi)^4} \text{tr} \{ [G_F^0(k)]^3 G_F^*(k) [G_F^0(q)]^3 \} \Delta^0(k - q) \right. \\
& + \frac{1}{2} g_s^2 \int \frac{d^4 k}{(2\pi)^4} \frac{d^4 q}{(2\pi)^4} \text{tr} \{ [G_F^0(k)]^3 G_F^*(k) [G_F^0(q)]^2 G_F^*(q) \} \Delta^0(k - q) \\
& \left. - i \int \frac{d^4 k}{(2\pi)^4} \text{tr} \{ [G_F^0(k)]^4 G_F^*(k) \Lambda_R^s(k) \} - i \int \frac{d^4 k}{(2\pi)^4} \text{tr} \{ [G_F^0(k)]^5 G_F^*(k) \Sigma_{RF}^s(k; M^* = M) \} \right], \tag{2.90}
\end{aligned}$$

where only the scalar terms are shown. Here Λ_R^s is the renormalized vacuum correction to the baryon-scalar vertex coming from scalar exchange, and $\Sigma_{RF}^s(k; M^* = M)$ is the renormalized scalar contribution to the baryon self-energy in the vacuum. [These functions are defined by Eqs. (A8), (A9), (A14), and (A21).] The vector contributions are completely analogous, except that the final two integrals contain Λ_R^v and $(-\gamma_\mu \Sigma_{RF}^v)$, while the first two terms enter with opposite sign and are proportional to g_v^2 . The first two integrals now contain the vector propagator $D^0(k - q)$, and γ_μ and γ^μ appear between the k -dependent and q -dependent baryon propagators. Since $\lim_{k \rightarrow \infty} \Sigma_{RF}^s(k) \sim k \ln(k^2)$ and $\lim_{k \rightarrow \infty} \Lambda_R^s(k) \sim \ln(k^2)$, it follows from power counting that all integrals in (2.90) are *finite*. We have thus arrived at a concise, finite expression for the two-loop vacuum fluctuation correction without explicitly evaluating any counterterms. This technique will clearly be useful if one wants to extend these results to higher orders in loops.

To express Eq. (2.90) in a form suitable for numerical computation, proceed as follows. First, evaluate the traces. Next, perform a Wick rotation to Euclidean space by defining $k_0 = ik_4$ and $q_0 = iq_4$. This is allowed because all poles in the integrands are determined by Feynman propagators.⁶⁸ The angular integrals can then be evaluated by introducing four-dimensional polar coordinates, with measure $d\Omega_4 = \sin^2\theta_2 d\theta_2 \sin\theta_1 d\theta_1 d\phi$, and using

$$\begin{aligned}
\int d^4 q \frac{1}{(k - q)^2 + m^2} & \equiv \frac{\pi^2}{k^2} \int_0^\infty q dq \Theta(k^2, q^2; m^2) \\
& = \frac{\pi^2}{k^2} \int_0^\infty q dq \{ k^2 + q^2 + m^2 - [(k^2 - q^2)^2 + 2m^2(k^2 + q^2) + m^4]^{1/2} \}, \tag{2.91}
\end{aligned}$$

$$\begin{aligned}
\int d^4 q \frac{kq}{(k - q)^2 + m^2} & \equiv \frac{\pi^2}{2k^2} \int_0^\infty q dq \Phi(k^2, q^2; m^2) \\
& = \frac{\pi^2}{2k^2} \int_0^\infty q dq \{ 2k^2 q^2 + (k^2 - q^2)^2 + 2m^2(k^2 + q^2) + m^4 \\
& \quad - (k^2 + q^2 + m^2)[(k^2 - q^2)^2 + 2m^2(k^2 + q^2) + m^4]^{1/2} \}, \tag{2.92}
\end{aligned}$$

where k and q are now Euclidean four-momenta. By changing variables to $y \equiv k^2$ and $z \equiv q^2$, the finite two-loop scalar contribution can be written as

$$\begin{aligned}
\mathcal{G}_{\text{VF}}^{(2)}(M^*) = & (M^* - M)^5 \frac{\gamma g_s^2}{8\pi^2} \left[\frac{1}{32\pi^2} \int_0^\infty dy \frac{y^2 - 3yM(M + M^*) + M^3 M^*}{(y + M^2)^3 (y + M^{*2})} [J_1(y; m_s^2) + J_3(y; m_s^2)] \right. \\
& + \frac{1}{64\pi^2} \int_0^\infty dy \frac{y(M^* + 3M) - M^2(M + 3M^*)}{(y + M^2)^3 (y + M^{*2})} [J_2(y; m_s^2) + J_4(y; m_s^2)] \\
& + \int_0^\infty dy \frac{y}{(y + M^2)^4 (y + M^{*2})} \left\{ y[y^2 - 2yM(3M + 2M^*) + M^3(M + 4M^*)] \frac{l_1^s(y)}{M} \right. \\
& \quad \left. - [y^2(M^* + 4M) - 2yM^2(2M + 3M^*) + M^4 M^*] l_2^s(y) \right\} \\
& + \int_0^\infty dy \frac{y}{(y + M^2)^5 (y + M^{*2})} \{ y[y^2(5M + M^*) - 10yM^2(M + M^*) \\
& \quad + M^4(M + 5M^*)] b_R^s(y) \\
& \quad - [y^3 - 5y^2 M(2M + M^*) \\
& \quad \left. + 5yM^3(M + 2M^*) - M^5 M^*] Ma_R^s(y) \} \right]. \tag{2.93}
\end{aligned}$$

The internal Euclidean integrals are defined by

$$J_1(y; m^2) = \frac{M}{2} \int_0^\infty dz \frac{3z - M^2}{(z + M^2)^3} \Theta(y, z; m^2), \quad (2.94)$$

$$J_2(y; m^2) = \frac{1}{2} \int_0^\infty dz \frac{z - 3M^2}{(z + M^2)^3} \Phi(y, z; m^2), \quad (2.95)$$

$$J_3(y; m^2) = \frac{1}{2} \int_0^\infty dz \frac{z(2M + M^*) - M^2 M^*}{(z + M^2)^2 (z + M^{*2})} \Theta(y, z; m^2), \quad (2.96)$$

$$J_4(y; m^2) = \frac{1}{2} \int_0^\infty dz \frac{z - M^2 - 2MM^*}{(z + M^2)^2 (z + M^{*2})} \Phi(y, z; m^2), \quad (2.97)$$

and the vertex functions (l_1^s and l_2^s) and self-energy functions (a_R^s and b_R^s) are defined in Appendix A.

For the vector contribution, the following changes must be made in Eq. (2.93). (i) Replace the overall factor of g_s^2 by g_v^2 . (ii) In the first two integrals, replace $1/32\pi^2$ by $(-1/8\pi^2)$ and $1/64\pi^2$ by $1/32\pi^2$. All the inner integrals are now $J_i(y; m_v^2)$. (iii) The vertex and self-energy functions should be replaced by l_1^v , l_2^v , a_R^v , and b_R^v , all of which are defined in Appendix A.

Thus the two-loop vacuum fluctuation term $\mathcal{E}_{\text{VF}}^{(2)}$ has been reduced to quadrature. Nevertheless, since the Euclidean integrals in (2.93) are over a semi-infinite domain, care is required to produce accurate numerical results. This is particularly true at high density, where small values of M^* lead to cancellations in the integrands. We found that an iterated Gaussian quadrature, split into two regions in each integral, produced results that were accurate to better than 0.1% with a moderate number of points (≈ 32 in each region). The largest uncertainty comes from the first two nested Euclidean integrals. The accuracy could be increased to roughly 0.03% by doubling the number of Gaussian points in each split region. These results were checked in an independent computer code by evaluating the J_i integrals analytically; this leaves only a single Euclidean integral that is much easier (and faster) to evaluate accurately. [We will be happy to supply the analytic expressions for the $J_i(y)$ on request.] The results were checked again by a third computer code that evaluated $\mathcal{E}_{\text{VF}}^{(2)}$ with the formulas in Appendix C. This verified both the algebra leading to Eq. (2.93) and the numerical accuracy; all three codes produced values for the energy density that agreed to four significant figures over the relevant density range.

Let us summarize the expressions that are used to obtain the numerical results in Sec. III. The total two-loop energy density $\mathcal{E}^{(2)}$ is given by Eq. (2.82), with $\mathcal{E}^{(1)}$ from (2.72) and (2.70). The two-loop contributions $\mathcal{E}_{\text{ex}}^{(2)}$, $\mathcal{E}_{\text{LS}}^{(2)}$, and $\mathcal{E}_{\text{VF}}^{(2)}$ are found in Eqs. (2.86), (2.88), and (2.93), respectively, with auxiliary quantities defined in Eqs. (2.89), (2.94)–(2.97), and Appendix A.

III. RESULTS

We now present numerical results for the two-loop energy computed with the equations in Sec. II. Since the

various two-loop corrections to the energy are additive [see Eq. (2.82)], it is sensible to isolate and examine different contributions (scalar exchange, vector vacuum fluctuations, etc.). First we consider a perturbative calculation in which the energy is evaluated using parameters and mean fields from the one-loop (RHA) calculation. We then minimize the full two-loop energy with respect to M^* and determine new parameters that reproduce the normalization conditions. To constrain the parameters, we take as our physical input the “empirical” saturation properties of nuclear matter, which we define as a binding energy of 15.75 MeV at an equilibrium density corresponding to $k_F = 1.3 \text{ fm}^{-1}$. We also fix the vector meson mass at the experimental ω meson mass⁵⁷ ($m_v = 783 \text{ MeV}$), leaving three free parameters (two coupling constants and the scalar meson mass).

A. Perturbative results

To test perturbative convergence, the two-loop energy is evaluated using RHA couplings and masses from Ref. 10 (see Table I) and the values of M^* that minimize the *one-loop* energy at each density. The RHA parameters were chosen so that nuclear matter equilibrium is at the empirical point, as defined above.⁵⁸

The nuclear matter binding curve for the perturbative two-loop calculation is compared to the corresponding curve for the one-loop energy in Fig. 4. To set the scale, we also show the MFT part of the one-loop energy defined by $\mathcal{E}^{(1)}(M^*, \rho_B) = \mathcal{E}_{\text{MFT}}(M^*, \rho_B) + \Delta\mathcal{E}(M^*)$. If the loop expansion were perturbatively convergent at the two-loop level, the two-loop corrections would not greatly alter the RHA saturation curve. Yet the full two-loop energy saturates at a density corresponding to $k_F = 2 \text{ fm}^{-1}$ with a binding energy of 400 MeV. Assessing the changes that occur from corrections can be difficult in QHD because of the different energy scales involved. In particular, the binding energy of nuclear matter is much smaller than the nucleon or meson masses or typical sizes of the mean fields. In this case, however, the corrections are large by any reasonable criterion.

Individual contributions to the energy per nucleon at the RHA equilibrium density ($k_F = 1.3 \text{ fm}^{-1}$) are shown in Fig. 5. The bars on the left correspond to the full two-loop energy (the dashed line in Fig. 4) while those on the right are for the one-loop energy (the solid line in Fig. 4). The one-loop energy $\mathcal{E}^{(1)}$ [Eq. (2.72)] is labeled RHA and $\mathcal{E}^{(1)} - \Delta\mathcal{E}$ is labeled MFT. The two-loop contributions are defined in Eq. (2.82) and are further separated into pieces proportional to the scalar and vector couplings. Recall that the exchange piece (ex) involves only the valence nucleons inside the Fermi sea, the Lamb shift

TABLE I. Walecka model parameters.

	g_s^2	m_s (MeV)	g_v^2	m_v (MeV)
MFT	109.6	520	190.4	783
RHA	54.3	458	102.8	783
Set A	183.0	893	55.0	783
Set B	290.0	1300	0.0	783

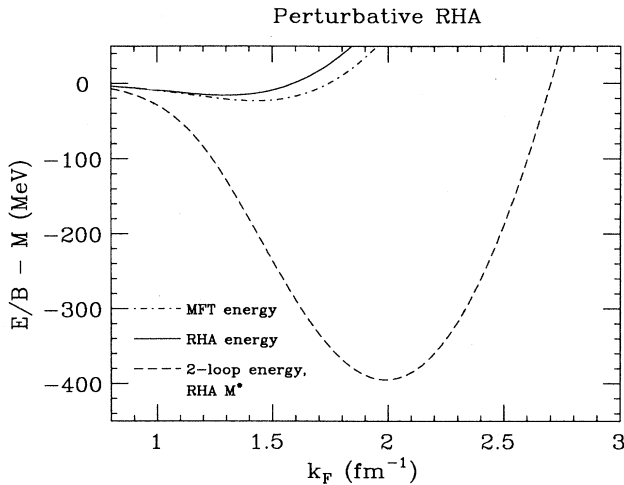


FIG. 4. Nuclear matter saturation curve for the mean-field (dot-dashed), one-loop (solid), and two-loop (dashed) energies, using RHA parameters and one-loop M^* .

(LS) arises from modifications to the valence nucleon spectrum from their interaction with meson fluctuations, and the vacuum fluctuations (VF) involve both virtual baryon and meson excitation.

Evidently, the new two-loop contributions are dominated by the strongly attractive vector Lamb shift and vacuum fluctuation terms, and their sum is comparable to the separate scalar and vector contributions to the mean-field energy. The exchange terms are relatively unimportant. The additional attraction overwhelms the sensitive cancellation of the MFT pieces at the empirical equilibrium point, driving saturation to higher density and much greater binding energy.

The M^* dependence of the vacuum fluctuation terms is $(M - M^*)^5$ times a function that varies by roughly 25% for $0 \leq M^* \leq M$, and for fixed M^* these terms scale like

the squares of the coupling constants. If calculated with equal meson masses and couplings, the vector contribution is approximately three times larger than the scalar and has opposite sign; for the RHA parameters in Table I, the vector contributions clearly dominate. As indicated by the figures, the net effect of these terms (and the Lamb shift contributions) will be too much attraction for values of the vector coupling used in previous QHD studies^{2,31} and for values implied by modern boson-exchange potentials.⁵⁹ As we will see, the vector coupling must be reduced significantly to prevent these pieces from dominating the energy.

If we try to minimize the two-loop energy with respect to M^* near nuclear matter density, so as to test strong convergence, we find no minima for positive M^* . To understand this situation, first consider the effective potential, which is the energy density at zero baryon density: $U_{\text{eff}}(M^*) \equiv \mathcal{E}(M^*, \rho_B = 0)$. The effective potential has a ϕ^2 piece from the classical (mean) field, a one-loop contribution $\Delta \mathcal{E}(M^*)$, and two-loop vacuum fluctuation contributions $\mathcal{E}_{\text{VF}}^{(2)}(M^*)$. By construction, the loop corrections behave as $(M^* - M)^5$ around $M^* = M$, so there is always a local minimum at $M^* = M$. (See Fig. 6.) At the one-loop level, the loop correction has an overall negative slope that makes the effective potential turn over at some $M^* > M$ and go to $-\infty$ as $M^* \rightarrow \infty$. This behavior is typical of one-loop effective potentials with fermions.²⁸

At the two-loop level, the new scalar (negative slope) and vector (positive slope) vacuum fluctuation contributions compete, so the relative size of couplings determines the overall behavior of the effective potential. As is evident from the figure, with RHA couplings, the two-loop effective potential goes to large negative values as $M^* \rightarrow 0$. Thus, with either one or two loops, the “vacuum” we work with is only a local minimum; the implications of living in a local minimum are addressed in Sec. IV.

What happens as the density is increased? In general, the overall slope of the energy density as a function of

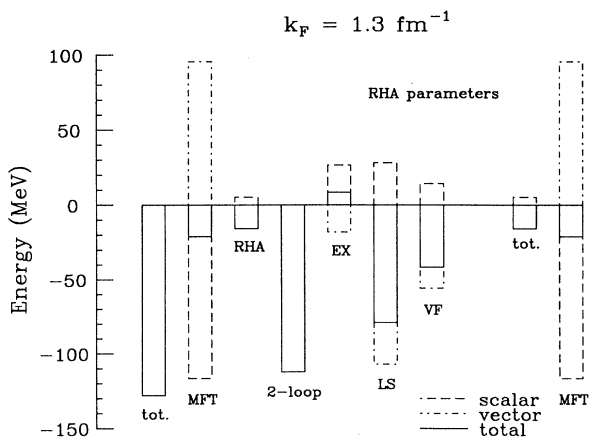


FIG. 5. Contributions to the two-loop (left) and one-loop (right) energies for the perturbative calculation (RHA parameters and one-loop M^*) at empirical nuclear matter saturation density ($k_F = 1.3 \text{ fm}^{-1}$).

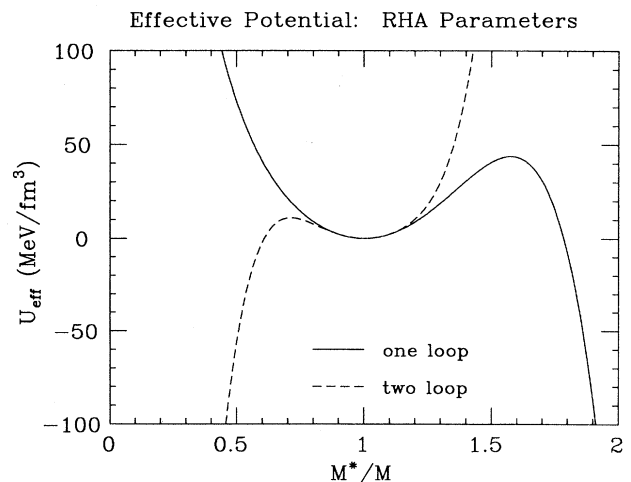


FIG. 6. One-loop and two-loop effective potentials as a function of M^* , using RHA parameters.

M^* becomes more positive (i.e., the curves in Fig. 6 “rotate” counterclockwise). In the RHA (one-loop), the local minimum moves toward lower M^* , further away from the maximum at $M^* > 1$, which slowly moves to larger M^* . At all densities there is a (locally) well-defined minimum, which occurs at a different M^* from the MFT minimum. With RHA parameters in the two-loop calculation, however, the local minimum becomes shallower as the density is increased and then *disappears completely* for $k_F \gtrsim 0.9 \text{ fm}^{-1}$. At higher densities, a new minimum appears at small positive M^* , but this corresponds to an unphysical solution with an acausal equation of state. Thus the two-loop corrections change the nature of the system *qualitatively*. This makes it impossible to compare the true two-loop corrections to the usual MFT or RHA solutions at high density (or even normal density). In any case, the expansion is not strongly convergent.

More information about the vacuum fluctuation terms, such as the relative importance of different (Euclidean) momentum regimes in the two-loop integrals, can be obtained by including a form factor at one of the meson-nucleon vertices in Fig. 1. Figure 7 shows the two-loop saturation curves with RHA parameters and a fixed cutoff of the form

$$f(q^2) = \frac{1}{1 + q^2/\Lambda^2}, \quad (3.1)$$

where q is a Euclidean momentum. We find that momenta up to 20 GeV make non-negligible contributions to the vacuum fluctuation integrals. Nevertheless, the low-momentum regime dominates, and even a 1 GeV Euclidean cutoff does not change the conclusion that corrections are large. (Using $\Lambda = 1 \text{ GeV}$ with RHA parameters reduces the scalar vacuum fluctuation contribution by a factor of 2 and the vector vacuum fluctuation contribution by a factor of 4. These become 20% and 40% reductions with $\Lambda = 2 \text{ GeV}$.) The low-momentum contributions from the vacuum fluctuation integrals, together

with the Lamb shift energy (with no form factor), still provide too much attraction. If a cutoff mass of $2M^*$ is used to simulate possible effects of higher-loop vertex corrections, the result is similar to the fixed 1 GeV cutoff. [We note that the actual behavior of such vertex corrections in the present model is not known. Since the Walecka model is not asymptotically free, however, (3.1) must be incorrect at very large momenta.]

B. Nonperturbative results and weak convergence

The loop expansion requires a minimization of the full two-loop energy with respect to M^* at each density. If we use RHA parameters, the two-loop energy near equilibrium density and higher has no minimum that describes a physical solution and so fails the test of strong convergence. However, we can try to satisfy the criterion of weak convergence by finding a *new* parameter set for which the two-loop energy can be minimized (at least locally) and which predicts nuclear matter saturation at the empirical values. In fact, a range of parameters can be found, since at the two-loop level there are three relevant constants to be determined (scalar and vector couplings and the scalar mass) and only two normalization conditions (binding energy and equilibrium density).

We present results for two parameter sets that indicate the range of possible parametrizations (see Table I). These sets feature the maximum (set *A*) and minimum (set *B*) values of the vector coupling compatible with empirical nuclear matter saturation. (We have not made an exhaustive search of the parameter space, but no hints of anything qualitatively different were found.) While the one-loop results depend only on the ratios of couplings to masses, the two-loop terms are sensitive to the masses and couplings separately. We find that in fitting parameters, the scalar mass provides the most leverage for adjusting the predicted saturation point.⁶⁰

With the new parameters, the nuclear matter saturation curves using the full two-loop energy are similar to the one-loop curve (see Fig. 8), although the compressibil-

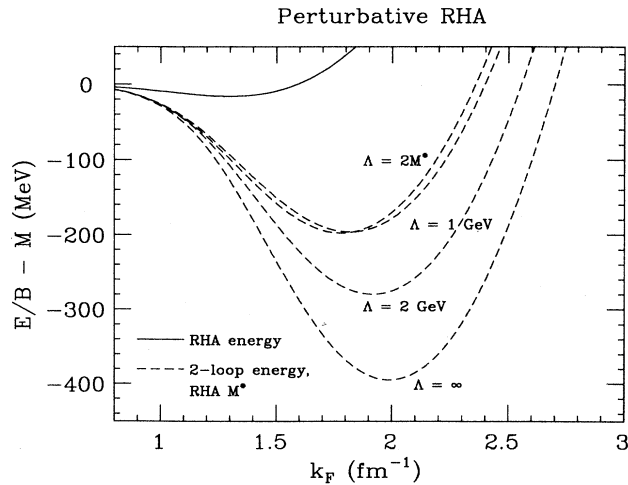


FIG. 7. Nuclear matter saturation curve as in Fig. 4, but including form factors in the two-loop vacuum fluctuation contributions.

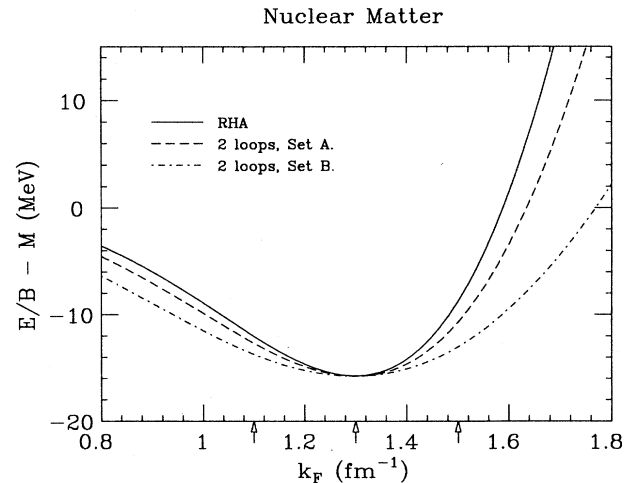


FIG. 8. Nuclear matter saturation curve for the RHA only (solid) and for the full two-loop energy using parameter sets *A* (dashed) and *B* (dot-dashed). The arrows indicate the densities shown in the histograms below.

ity for set B is considerably lower. (At equilibrium, set A predicts a compressibility of 348 MeV with $M^*/M=0.78$, while set B predicts 206 MeV and $M^*/M=0.88$.) Nevertheless, the qualitative features of the two-loop description are very different from the one-loop physics. In essence, the parameters are finely tuned to minimize corrections from the quantum vacuum at the two-loop level. This fine tuning requires a drastic reduction of the vector meson coupling (even to zero) and a significant increase in both the scalar coupling and mass, compared to the one-loop parameters. We remark that Nyman and Rho required similar fine tuning to reduce the loop corrections in the σ model; this was achieved by a similar increase in the scalar mass.^{34,35}

The qualitative changes in the physics with the new two-loop parameter sets are evident from Fig. 9, in which we plot Yukawa potentials using the parameter sets from Table I. These curves indicate the effective nonrelativistic NN interaction obtained in the one-boson-exchange approximation with very heavy baryons. The intuitive relationship between vector exchange and short-range repulsion and between scalar exchange and midrange attraction is apparently lost with parameters that reproduce nuclear matter saturation at the two-loop level.⁶¹ It is still possible that the NN interaction obtained from the two-loop effective action resembles the Yukawa potential seen in the MFT, with short-range repulsion and midrange attraction; nevertheless, the origin of these forces would be quite different.

Individual contributions to the two-loop energy are shown in Figs. 10 and 11 for several densities near equilibrium, together with the one-loop results with RHA parameters as in Fig. 5. These figures allow us to identify the interplay between the different pieces of the energy and to see how this interplay changes *qualitatively* when the parameters are refitted with the two-loop corrections.

As is evident from the right-hand side of the figures, the one-loop calculations (with RHA parameters) achieve

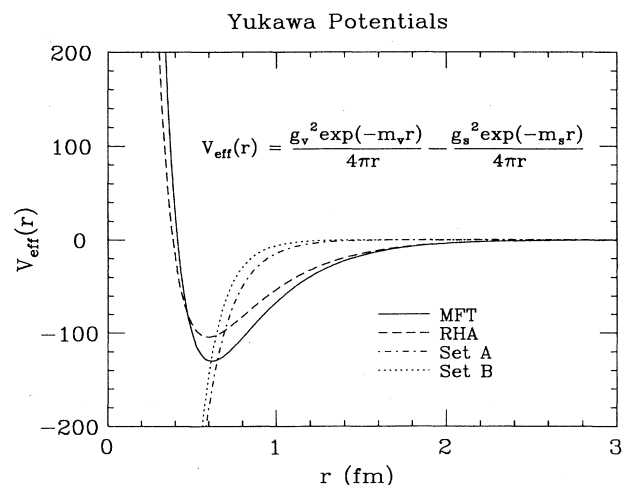


FIG. 9. Yukawa potentials (in MeV) illustrating the nature of the NN interaction in a one-boson-exchange picture, using parameter sets A and B and parameters from the MFT and RHA (see Table I).

saturation through a delicate density-dependent balance of vector repulsion and scalar attraction. The one-loop vacuum correction is small but significant on the scale of the binding energy.

With the new parameters, the picture changes in three essential ways. First, the corrections from the quantum vacuum (Lamb shift and vacuum fluctuation pieces) are

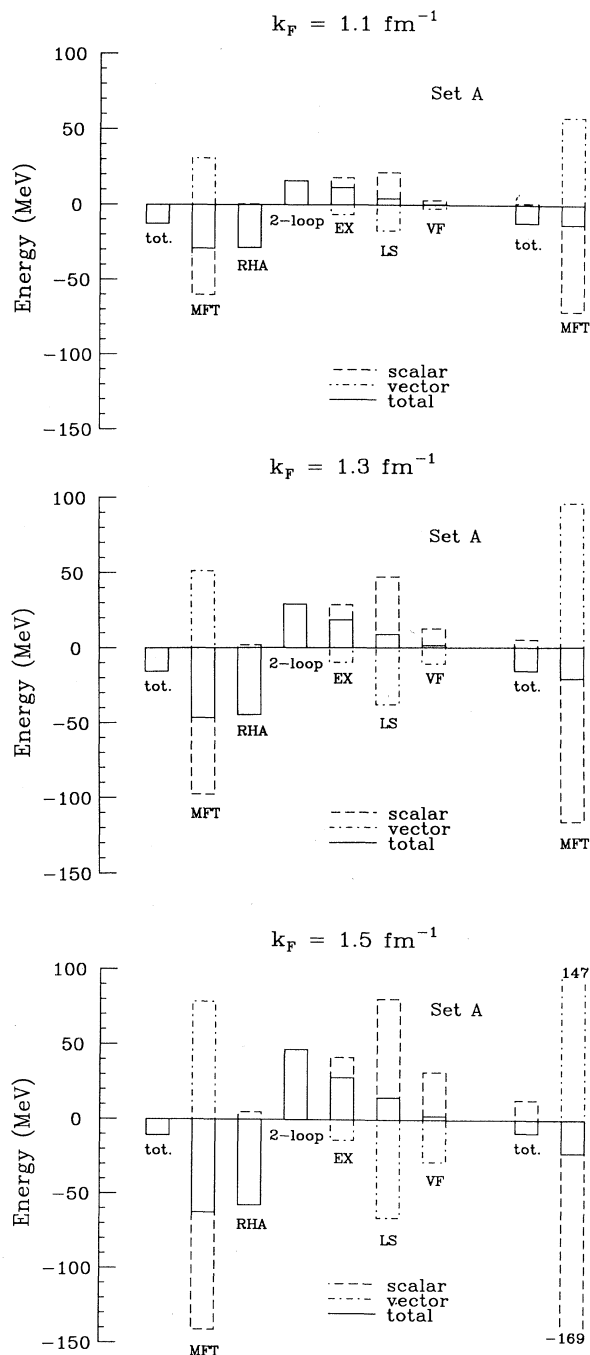


FIG. 10. Contributions to the two-loop energy near nuclear matter saturation for parameter set A , as in Fig. 5. The one-loop energy with RHA parameters is represented by the bars on the right.

reduced, either directly (by increasing the scalar mass) or through cancellations (by decreasing the vector coupling). Moreover, the individual scalar and vector one-loop contributions are smaller than before, but their cancellation is less complete, leading to significant overbinding if we consider these terms alone. Finally, however, the two-loop contributions are now significantly repulsive, as they

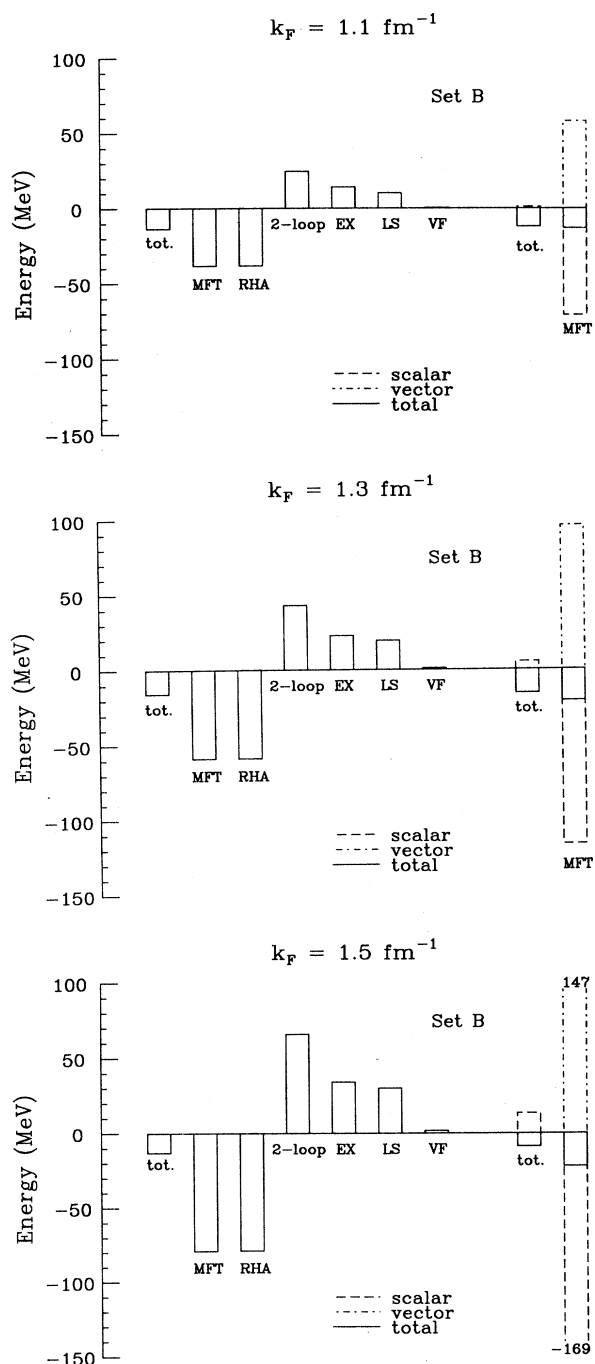


FIG. 11. Contributions to the two-loop energy near nuclear matter saturation for parameter set *B*, as in Fig. 5. The one-loop energy with RHA parameters is represented by the bars on the right.

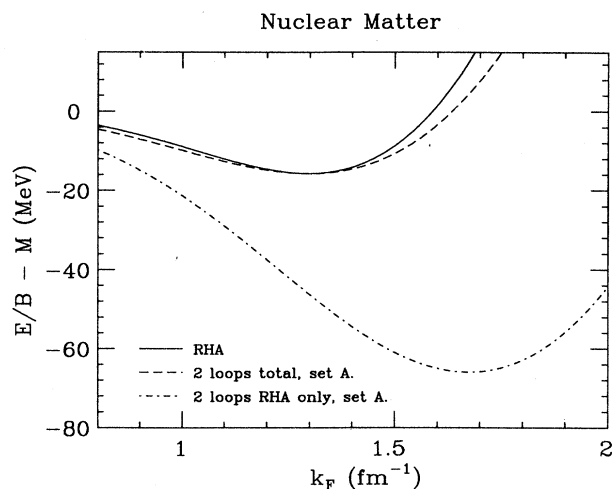


FIG. 12. Nuclear matter saturation curve for the RHA only (solid) and for the full two-loop energy using parameter set *A* (dashed), as in Fig. 4. The dot-dashed curve is the one-loop contribution to the dashed curve.

are dominated by the scalar exchange terms. The two-loop vacuum fluctuations are essentially negligible, and the Lamb shift is a small but relevant contribution that also reduces the binding.

Nuclear matter saturation in the two-loop calculation is thus achieved almost entirely from the dynamics of scalar-meson exchange and, in particular, from an interplay of attractive mean-field contributions and repulsive two-loop scalar terms (both exchange and Lamb shift) that involve occupied states in the Fermi sea. In Fig. 12 the one-loop contributions to the energy for set *A* are isolated to illustrate the large energy scale of this interplay. Furthermore, as demonstrated by set *B*, it is possible to reproduce nuclear matter saturation with no vector meson at all.

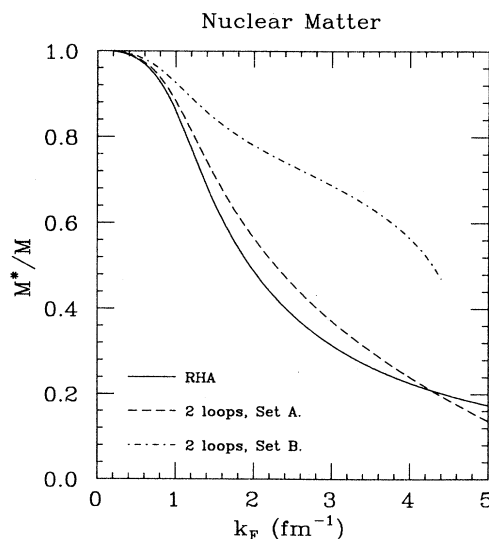


FIG. 13. Nucleon effective mass as a function of the Fermi momentum for the RHA and the two-loop calculations with parameter sets *A* and *B*.

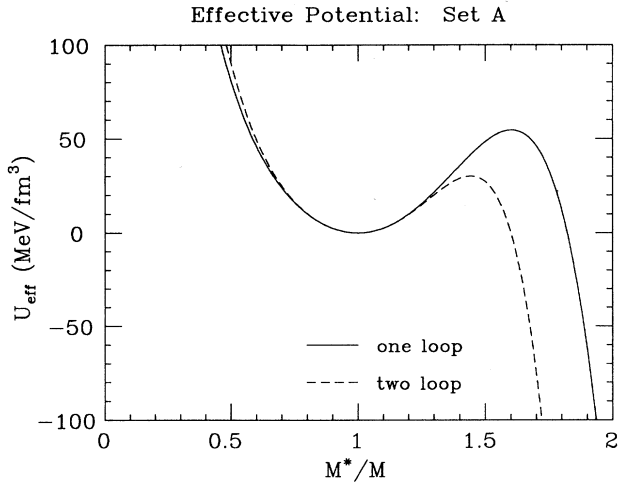


FIG. 14. One-loop and two-loop effective potentials as a function of M^* , using parameter set A .

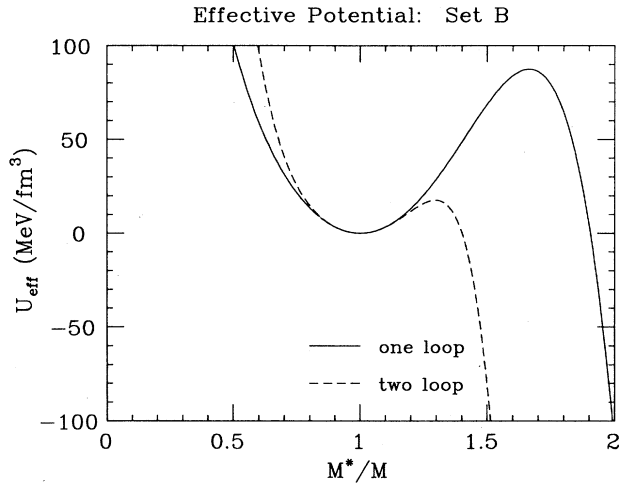


FIG. 15. One-loop and two-loop effective potentials as a function of M^* , using parameter set B .

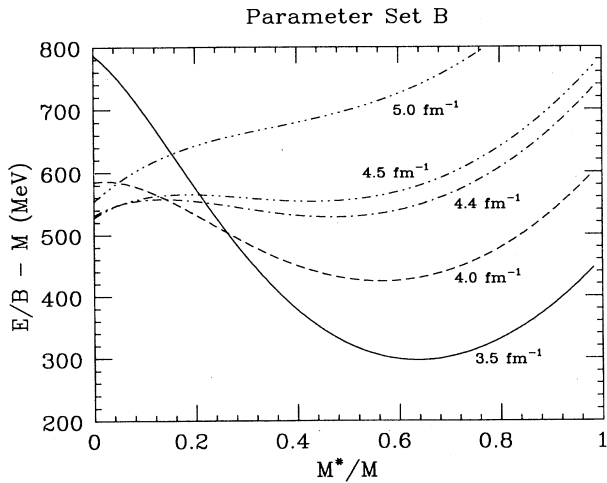


FIG. 16. Two-loop energy as a function of M^* , using parameter set B , for a range of densities. The curves are labeled by the value of k_F .

The behavior of the effective mass as a function of density is shown in Fig. 13 for the one-loop calculation (RHA parameters) and the two-loop calculations with parameter sets A and B . The RHA curve starts at the nucleon mass at low density, drops rapidly near the equilibrium density, and then smoothly approaches zero at high density. The curve for set A is qualitatively similar for the range of densities in the figure. However, at $k_F \approx 7 \text{ fm}^{-1}$, it passes through $M^*=0$. The curve for set B decreases abruptly and terminates near $k_F=4.5 \text{ fm}^{-1}$, where the energy can no longer be minimized for positive M^* .

We can understand this behavior by considering the energy density as a function of M^* , starting with zero density (the effective potential). Figures 14 and 15 show that the one-loop and two-loop effective potentials for sets A and B are qualitatively similar, although the two-loop local minimum at $M^*=M$ is not as isolated as the one-loop minimum. As the density increases, this minimum in the energy becomes more pronounced with respect to the local maximum at $M^*>1$, but eventually the two-loop corrections bring the curve down at small M^* , producing a new local minimum. For set B , the original minimum in the energy disappears above 4.5 fm^{-1} , as shown in Fig. 16, while for set A the minimum moves continuously to negative M^* . The implications for the validity of the MFT at high densities are discussed in the next section.

IV. DISCUSSION

The results of Sec. III demonstrate that two-loop corrections in the Walecka model produce large quantitative changes in the description of nuclear matter if the parameters are held fixed and large qualitative changes in the physics if they are adjusted to reproduce empirical saturation properties. Thus the loop expansion (through two-loop order) is neither strongly nor weakly convergent.

To understand these results in general terms, it is useful to focus on $\mathcal{E}(M^*, \rho_B)$ as a function of both M^* and ρ_B . A clear discussion of the effective potential is given by Coleman and Weinberg,²² and we can generalize their treatment to the present case. In the Walecka model, the effective potential in the MFT is simply $\frac{1}{2}m_s^2\phi^2$ and thus has an absolute minimum at $\phi=0$ or $M^*=M$. When the one-loop corrections are added, the renormalization conditions on the potential ensure that this minimum survives, but as is clear from Fig. 6, the minimum is now local. As discussed by Coleman and Weinberg, however, when the loop corrections to the MFT are large, it is reasonable to expect that neglected higher-order corrections are (at least) comparable. Even where the one-loop corrections are small, higher-order corrections may be large, because the loop expansion is perturbative in the large couplings.

In any case, the one-loop corrections can be valid only where they are small, namely, near the local minimum of the effective potential. Fortunately, this regime is sufficient because the RHA and MFT effective potentials are close to one another for the range of scalar field

strengths needed to study nuclear matter. Since the overall slope of the effective potential is negative, increasing the density improves the status of the local minimum, and physical one-loop solutions exist at all densities; it is easy to verify that no other local minima exist in the Walecka-model RHA. Moreover, although the location of the RHA minimum at various densities differs from that found in the MFT, the resulting RHA description is not qualitatively different from the MFT, and as has been emphasized repeatedly,² the RHA equation of state approaches that of the MFT in the high-density limit.

When the two-loop corrections are included using the RHA parameters, several important changes occur. Although the local minimum at $M^* = M$ remains intact (as guaranteed by the renormalization conditions), it becomes less pronounced, and the regime where the loop corrections are small is reduced. This is certainly not characteristic of a convergent expansion, in which higher-order corrections would presumably enlarge the regime of applicability. It could even imply that the loop expansion has no regime of applicability, and that further loop corrections will produce an increasingly unstable situation. In addition, since the attractive vector contributions dominate, the overall slope of U_{eff} is now positive. Increasing the density causes the local minimum to disappear before equilibrium nuclear matter density is reached, precluding a comparison between the high-density two-loop equation of state and that of the MFT.

This disaster can be avoided by readjusting the parameters to reduce the vacuum corrections, which allows the local minimum to be maintained through the regime of normal density. With the new parameters, one finds an effective potential that qualitatively resembles the one-loop result, as shown in Figs. 14 and 15. Unfortunately, the results are still unsatisfactory for two reasons. First, the new parameters imply a qualitatively different picture of the nucleon-nucleon interaction from that obtained at the one-loop level. In addition, at high enough density, the local minimum disappears anyway (Fig. 16), and any new minimum that develops occurs outside the region of applicability, since it is generated by large two-loop corrections. Thus, even though the high-density two-loop equation of state resembles that of the MFT (since the energy is dominated by M^* -independent terms), the comparison is questionable because the validity of the two-loop solution is questionable. We are therefore forced to conclude that the loop expansion is not even weakly convergent through two-loop order.

Could the two-loop problems be cured by introducing additional (nonlinear) scalar interactions, such as in the chiral σ model? Given the results of previous calculations,³⁴⁻³⁶ this appears unlikely. In all calculations to date, fine tuning³⁵ and parameters similar to the new sets found here⁶² were required to achieve reasonable results. In fact, difficulties found here at the two-loop level occur in the σ model already at the mean-field and one-loop levels.^{63,64} More importantly, the vector meson loops (which have not been studied in any of the previous work) produce the most serious problems, and it is difficult to argue that some *a priori* cancellation exists between vector and scalar terms, even in a chiral model.

The failure of the loop expansion is, perhaps, not surprising. As is clear from Eq. (2.57), the two-loop corrections are essentially *perturbative* corrections to the one-loop results; the nonperturbative aspects reside solely in the determination of the new mean field. In the loop expansions performed by Coleman and Weinberg²² and by Lee and Wick,²⁸ the couplings were assumed to be small. Unfortunately, in regimes relevant for nuclear physics, the couplings in hadronic relativistic field theories are large. This leaves open the strong possibility that there are important corrections to the RHA that are not included efficiently in the loop expansion. These corrections could reduce the effective strength of the interaction, particularly in the vacuum loops. These considerations are especially important for calculations at low density (e.g., the effective potential), since even a reasonable starting point is not known in this regime. There is no reason at all to believe that the loop expansion is meaningful at low density for large couplings.

Thus the failure of the loop expansion encountered here does not necessarily imply that the MFT and RHA results are inaccurate representations of the underlying quantum field theory. These simple approximations may still be useful starting points for computing corrections in QHD, especially at high density. We have simply found that the loop expansion is apparently not a good way to obtain these corrections.⁶⁵

Though there may be good explanations and interpretations of the unfavorable two-loop results, we are nevertheless forced to reconsider and reassess the QHD approach. Let us start by reviewing the advantages. QHD is a consistent framework for studying hadronic physics: The dynamical assumptions are made at the outset, and one then attempts to extract concrete results from the implied formalism. Since QHD is based on local, Lorentz invariant lagrangian densities, causality and covariance can be maintained. There are no *theoretical* limitations to using this approach at large energy and momentum transfers (although the results may disagree with nature). In addition, the relevance of mesonic degrees of freedom in nuclear systems is well established, and hadronic degrees of freedom are efficient. Other effects, such as relativity and the dynamics of the vacuum, which are still controversial, can be investigated systematically. Finally, this approach has the virtue that it can fail.

In QHD models with renormalizable Lagrangians, the number of parameters is finite; once they are determined by an appropriate set of empirical data, subsequent predictions are finite and unambiguous. Calculations can be extended beyond the tree level in a systematic fashion, and we can study the quantum vacuum without introducing additional parameters determined solely by short-distance phenomena. The dynamical assumption underlying renormalizability is that the short-distance behavior and the quantum vacuum can be described in terms of hadronic degrees of freedom only. This assumption must ultimately break down, since hadrons are actually composed of quarks and gluons. We must therefore minimize the sensitivity of calculated results to short-distance physics.

Renormalizable QHD theories allow us to study if and

where and how hadronic degrees of freedom are adequate for calculations beyond the tree level. Although most calculations in QHD have stopped at the one-loop level, some QHD calculations have been carried out in more “refined” approximations (such as Dirac-Hartree-Fock or Dirac-Brueckner) that are motivated by the corresponding nonrelativistic approximations. The reliability of these approximations has not been studied, in part because they have not been formulated in ways that make systematic improvement practical. These systematic studies are crucial for interpreting the successes of the simple calculations and for investigating the claim that the MFT becomes exact at high density.

If QHD must fail at short distances, why not apply QCD directly? In principle this is desirable, but in practice there are many difficulties. While QCD is believed to be the theory of the strong interaction, its consequences for nuclear physics have only been explored indirectly using “QCD-inspired” models. Actual QCD predictions at nuclear length scales with the precision of existing (and anticipated) data are not presently available, and this state of affairs will probably persist for some time. Even if it becomes possible to use QCD to describe many-nucleon systems, this description is likely to be awkward, since quarks cluster into hadrons at low energies, and hadrons are the degrees of freedom actually observed in experiments. It is thus extremely important to see if practical and reliable hadronic descriptions can be developed for the energy, density, and temperature regimes available in the new experimental facilities. In addition, to discover essential manifestations of quark/gluon degrees of freedom in nuclear systems, we must push hadronic descriptions to their limits and find concrete failures.

The purpose of this work was to investigate the loop expansion as a method for computing reliably in QHD. While it appears that this expansion is not useful, it may be that the two-loop results provide an accurate picture of the field theory and that all higher-loop corrections are small. Even a qualitative investigation of the three-loop terms should resolve this question. If we assume that the loop expansion cannot be rescued, then we must search for alternatives; these are needed to justify the phenomenological successes of the MFT and RHA, or to relegate them to pure phenomenology. The calculations presented here make two things reasonably clear: First, a useful expansion scheme (if it exists) must reduce the importance of the vacuum corrections that enter beyond one-loop order. Second, as is clear from Eq. (2.57), it is likely that the RHA will serve as a starting point in any successful scheme, since it allows us to incorporate the mean fields in the propagators. Moreover, in any scheme for calculating corrections to the RHA, the corresponding mean fields can be determined *at the end of the calculation* by extremizing the energy density. The difficult part is deciding how to group the corrections contained in the final two exponentials of Eq. (2.57). This will not be an easy task, since the simplest (perturbative) grouping is not useful. The burden is on the QHD practitioners to discover viable alternatives.

ACKNOWLEDGMENTS

We are pleased to thank our colleagues T. D. Cohen, C. J. Horowitz, M. H. Macfarlane, D. P. Murdock, J. D. Walecka, and G. E. Walker for valuable discussions and comments. One of us (R.J.P.) acknowledges a Presidential Young Investigator Award from The National Science Foundation and a seed grant from The Ohio State University Office of Research and Graduate Studies. This work was also supported in part by the National Science Foundation under Grant Nos. PHY-8719526 and PHY-8858250 and by the U.S. Department of Energy under Contract Nos. DE-FG05-87ER40322 and DE-FG02-87ER40365.

APPENDIX A: BARYON SELF-ENERGY AND BARYON-SCALAR VERTEX

Here we derive results for the baryon self-energy and vertex that are needed to perform the calculations in Sec. II. We consider only the exchange contributions to the self-energy, as indicated in Fig. 17, since the direct terms are proportional to the mean meson fields and are automatically included in the baryon propagator when the effective action is extremized. Similarly, the relevant vertex diagrams involve scalar and vector exchange modifications to the bare baryon-scalar vertex, as shown in Fig. 18.

In general, in the presence of the mean fields, the exchange self-energy must be computed using the Hartree propagator G^H of Eq. (2.60). For the diagrams in Fig. 17, an application of the Feynman rules (see Fig. 29 of Ref. 2) leads to

$$\Sigma(k^*) \equiv \Sigma^s(k^*) - \gamma_\mu \Sigma^{v\mu}(k^*) \quad (\text{A1})$$

$$\begin{aligned} &= ig_s^2 \int \frac{d^4q}{(2\pi)^4} G^H(q) \Delta^0(k-q) \\ &\quad - ig_v^2 \int \frac{d^4q}{(2\pi)^4} \gamma_\mu G^H(q) \gamma^\mu D^0(k-q) \\ &= ig_s^2 \int \frac{d^4q}{(2\pi)^4} G^*(q) \Delta^0(k^*-q) \\ &\quad - ig_v^2 \int \frac{d^4q}{(2\pi)^4} \gamma_\mu G^*(q) \gamma^\mu D^0(k^*-q). \end{aligned} \quad (\text{A2})$$

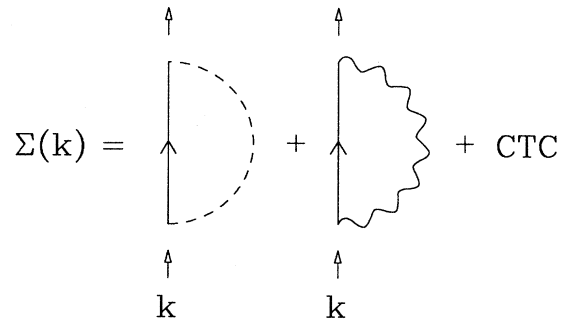


FIG. 17. Exchange contributions to the baryon self-energy Σ . The solid line represents the baryon Hartree propagator G^H , and the dashed and wiggly lines are scalar and vector propagators, respectively. The counterterm contributions (CTC) are discussed in the text.

$$ig_s(1+\Lambda) = \cdot + \text{[Diagram 1]} + \text{[Diagram 2]} + \text{CTC}$$

FIG. 18. Exchange corrections to the scalar-baryon-baryon vertex. The dot represents the bare vertex ig_s , and the propagators are defined as in Fig. 17. The counterterm contribution is given in Fig. 20.

Here $k^{*\mu} \equiv k^\mu - g_v V_e^\mu$ and we have dropped the longitudinal $k_\mu k_\nu$ term in the vector propagator, since it does not contribute to the energy density. Note that the baryon propagators contain both Feynman and density-dependent pieces, and dimensional regularization has been used to shift integration variables. This allows us to use the simpler propagator $G^*(q)$ and also emphasizes the dependence of the self-energy on the vector field, since V_e^μ now appears in the argument of the meson propagators.

Although Eq. (A2) is required for general applications, the energy density involves only closed loops. Thus, as discussed in Sec. II, the dependence on the vector field

can be shifted away (after dimensional regularization), so that the energy density depends only on $\Sigma(k)$, as is clear from Eqs. (2.83), (2.84), and (2.90). This occurs because we shift momenta in *two* baryon propagators, and the meson propagators depend only on the momentum difference. Moreover, the distinction between k and k^* is irrelevant for computing counterterms, since these are defined by vacuum conditions, where $V_e^\mu = 0$.

The density-dependent parts of the self-energy [defined by using only G_D^* in Eq. (A2)] are easily calculated:

$$\Sigma_D^s(k) = -g_s^2 \int \frac{d^3q}{(2\pi)^3} \frac{n_q^0}{2E^*(q)} \times \left[\frac{\gamma_0 E^*(q) - \boldsymbol{\gamma} \cdot \mathbf{q} + M^*}{[k_0 - E^*(q)]^2 - (\mathbf{k} - \mathbf{q})^2 - m_s^2} \right], \quad (\text{A3})$$

$$\gamma_\mu \Sigma_D^{v\mu}(k) = 2g_v^2 \int \frac{d^3q}{(2\pi)^3} \frac{n_q^0}{2E^*(q)} \times \left[\frac{\gamma_0 E^*(q) - \boldsymbol{\gamma} \cdot \mathbf{q} - 2M^*}{[k_0 - E^*(q)]^2 - (\mathbf{k} - \mathbf{q})^2 - m_v^2} \right], \quad (\text{A4})$$

where $E^*(q) \equiv (q^2 + M^{*2})^{1/2}$ and $n_q^0 \equiv \theta(k_F - |\mathbf{q}|)$. Substitution of these results into Eq. (2.83) yields (2.86).

The Feynman parts of the self-energy are

$$\Sigma_F(k) = \Sigma_F^s(k) - \gamma_\mu \Sigma_F^{v\mu}(k), \quad (\text{A5})$$

$$\begin{aligned} \Sigma_F^s(k) &= ig_s^2 \int \frac{d^\tau q}{(2\pi)^\tau} G_F^*(q) \Delta^0(k-q) \\ &= -\frac{g_s^2}{16\pi^2} \Gamma(2-\tau/2) \int_0^1 dx \frac{M^* + x\gamma_\mu k^\mu}{[M^{*2}(1-x) + m_s^2 x - k^2 x(1-x)]^{2-\tau/2}}, \end{aligned} \quad (\text{A6})$$

$$\begin{aligned} \gamma_\mu \Sigma_F^{v\mu}(k) &= ig_v^2 \int \frac{d^\tau q}{(2\pi)^\tau} \gamma_\mu G_F^*(q) \gamma^\mu D^0(k-q) \\ &= \frac{g_v^2}{8\pi^2} \Gamma(2-\tau/2) \int_0^1 dx \frac{x\gamma_\mu k^\mu - 2M^*}{[M^{*2}(1-x) + m_v^2 x - k^2 x(1-x)]^{2-\tau/2}}. \end{aligned} \quad (\text{A7})$$

Here we have introduced Feynman parameter integrals to combine denominators, and the τ -dimensional integrals follow from standard formulas of dimensional regularization. (See Ref. 47 or Appendix B of Ref. 2.) Notice that the logarithmic divergences now appear as poles in the Γ function at the physical dimension $\tau=4$.

To produce finite expressions for Σ_F^s and $\gamma_\mu \Sigma_F^{v\mu}$, the divergences must be removed by renormalization. To isolate the divergences, one can expand G_F^* around $M^* = M$ by noting that $G_F^* \rightarrow G_F^0$ when $M^* = M$ and by using the identity $\partial G_F^0(k)/\partial M = [G_F^0(k)]^2$. It follows from power counting that only the first two terms in this expansion diverge, as indicated in Fig. 19, and thus to renormalize the self-energy at finite density, one must add mass, wave-function, and vertex counterterms of the form in Eq. (2.78). The vertex correction involves only the vacuum propagator G_F^0 , and since the scalar field is

constant, the vertex is needed only at zero momentum transfer. It is given by

$$\begin{aligned} \Lambda(k) &= \frac{\partial}{\partial M} [\Sigma_F^s(k; M^* = M) - \gamma_\mu \Sigma_F^{v\mu}(k; M^* = M)] \\ &\equiv \Lambda^s(k) + \Lambda^v(k), \end{aligned} \quad (\text{A8})$$

which agrees with the results obtained by a direct application of the Feynman rules. (An overall factor of ig_s has been removed.)

The counterterms of Eq. (2.78) are now defined by imposing familiar vacuum renormalization conditions on the baryon propagator and vertex.^{15,66} Using the Feynman rules for the counterterms indicated in Fig. 20, the renormalized vacuum exchange self-energy can be written to second order in the couplings as

FIG. 19. Expansion of the exchange contributions to the baryon self-energy. The heavy solid line is the modified Feynman propagator G_F^* , and the thin solid line is the noninteracting Feynman propagator G_F^0 . The crosses represent factors of $(M^* - M) = -g_s \phi$. Only the scalar contributions are shown, but there are identical graphs involving vector-meson exchange.

$$\Sigma_{RF}(k; M^* = M) = \Sigma_F(k; M^* = M) - M_c + \zeta_N(\gamma^\mu k_\mu - M). \quad (\text{A9})$$

From our previous expansion, it is clear that only the second-order counterterms are needed to renormalize the self-energy. The counterterms are chosen so that the vacuum baryon propagator has a pole at $\gamma^\mu k_\mu = M$ with unit residue when the exchange correction is included. This implies

$$M_c \equiv \Sigma_F(k; M^* = M) \Big|_{\gamma^\mu k_\mu = M}, \quad (\text{A10})$$

$$\zeta_N \equiv - \left[\frac{\gamma^\mu k_\mu + M}{k^2 - M^2} [\Sigma_F(k; M^* = M) - M_c] \right] \Big|_{\gamma^\mu k_\mu = M}. \quad (\text{A11})$$

To evaluate the counterterms, it is convenient to define $\Sigma_F(k; M^* = M) \equiv Ma(k^2) - \gamma^\mu k_\mu b(k^2)$, where a and b can be deduced from Eqs. (A6) and (A7). It is then a straightforward matter of algebra to compute the counterterms in τ dimensions and subtract them from the vac-

FIG. 20. Feynman rules for the mass (M_c), wave-function (ζ_N), and vertex (γ_s) counterterms.

uum self-energy, producing a finite result for $\Sigma_{RF}(k; M^* = M)$ as $\tau \rightarrow 4^-$.

This procedure is, of course, insufficient to render $\Sigma_{RF}(k)$ finite for $M^* \neq M$. We must also add the vertex counterterm, which is defined by

$$g_s \Lambda(\gamma^\mu k_\mu = M, k^2 = M^2) + \gamma_s = 0. \quad (\text{A12})$$

This condition ensures that the baryon-scalar coupling is unchanged by the exchange corrections when the momentum transfer from the external scalar meson is zero. As with the other vertex counterterms [see the discussion following Eq. (2.70)], this definition produces the simplest expression for the energy density, but other choices of renormalization point (for example, at momentum transfer $q^2 = m_s^2$) are allowed.

The vertex counterterm can be calculated from Eqs. (A6)–(A8), and it enters in the definition of the renormalized Feynman self-energy at finite density [compare Eq. (A9)]:

$$\begin{aligned} \Sigma_{RF}(k) &= \Sigma_F(k) - M_c + \zeta_N(\gamma^\mu k_\mu - M) \\ &\quad - (M - M^*)\gamma_s / g_s \\ &= \Sigma_{RF}^s(k) - \gamma_\mu \Sigma_{RF}^{v\mu}(k), \end{aligned} \quad (\text{A13})$$

where

$$\begin{aligned} \Sigma_{RF}^s(k) &= \frac{g_s^2}{16\pi^2} \left[\int_0^1 dx (M^* + x\gamma^\mu k_\mu) \ln \left[\frac{M^{*2}(1-x) + m_s^2 x - k^2 x(1-x)}{M^2(1-x)^2 + m_s^2 x} \right] \right. \\ &\quad \left. + 2M^2(\gamma^\mu k_\mu - M) \int_0^1 dx \frac{x(1-x^2)}{M^2(1-x)^2 + m_s^2 x} + 2M^2(M - M^*) \int_0^1 dx \frac{1-x^2}{M^2(1-x)^2 + m_s^2 x} \right], \end{aligned} \quad (\text{A14})$$

$$\begin{aligned} \gamma_\mu \Sigma_{RF}^{v\mu}(k) &= \frac{g_v^2}{8\pi^2} \left[\int_0^1 dx (2M^* - x\gamma^\mu k_\mu) \ln \left[\frac{M^{*2}(1-x) + m_v^2 x - k^2 x(1-x)}{M^2(1-x)^2 + m_v^2 x} \right] \right. \\ &\quad \left. + 2M^2(\gamma^\mu k_\mu - M) \int_0^1 dx \frac{x(1-x)(2-x)}{M^2(1-x)^2 + m_v^2 x} + 2M^2(M - M^*) \int_0^1 dx \frac{(1-x)(2-x)}{M^2(1-x)^2 + m_v^2 x} \right]. \end{aligned} \quad (\text{A15})$$

These expressions are used in the evaluation of the Lamb shift $\mathcal{E}_{LS}^{(2)}$ in Eq. (2.88).

To evaluate the vacuum fluctuation correction $\mathcal{E}_{VF}^{(2)}$, the renormalized self-energy is needed only at $M^* = M$ and can be written as

$$\Sigma_{RF}(k; M^* = M) = M \{ g_s^2 a_R^s(k^2) + g_v^2 a_R^v(k^2) \} - \gamma^\mu k_\mu \{ g_s^2 b_R^s(k^2) + g_v^2 b_R^v(k^2) \}, \quad (\text{A16})$$

$$a_R^s(y) = \frac{1}{16\pi^2} \int_0^1 dx \left[\ln \left[\frac{M^2(1-x) + m_s^2 x + yx(1-x)}{M^2(1-x)^2 + m_s^2 x} \right] - \frac{2M^2 x(1-x^2)}{M^2(1-x)^2 + m_s^2 x} \right], \quad (\text{A17})$$

$$b_R^s(y) = \frac{-1}{16\pi^2} \int_0^1 dx \left[x \ln \left[\frac{M^2(1-x) + m_s^2 x + yx(1-x)}{M^2(1-x)^2 + m_s^2 x} \right] + \frac{2M^2 x(1-x^2)}{M^2(1-x)^2 + m_s^2 x} \right], \quad (\text{A18})$$

$$a_R^s(y) = \frac{-1}{4\pi^2} \int_0^1 dx \left[\ln \left[\frac{M^2(1-x) + m_v^2 x + yx(1-x)}{M^2(1-x)^2 + m_v^2 x} \right] - \frac{M^2 x(1-x)(2-x)}{M^2(1-x)^2 + m_v^2 x} \right], \quad (\text{A19})$$

$$b_R^s(y) = \frac{-1}{8\pi^2} \int_0^1 dx \left[x \ln \left[\frac{M^2(1-x) + m_v^2 x + yx(1-x)}{M^2(1-x)^2 + m_v^2 x} \right] - \frac{2M^2 x(1-x)(2-x)}{M^2(1-x)^2 + m_v^2 x} \right]. \quad (\text{A20})$$

Here we have replaced the square of the Minkowski momentum with the square of the Euclidean momentum: $k^2 = -y$. These expressions are used in Eq. (2.93).

Finally, the contributions from the vacuum vertex corrections, which are also needed in Eq. (2.93), are given by

$$\Lambda_R(k) \equiv \Lambda(k) + \gamma_s / g_s = \frac{\gamma^\mu k_\mu}{M} [g_s^2 l_1^s(k^2) + g_v^2 l_1^v(k^2)] + g_s^2 l_2^s(k^2) + g_v^2 l_2^v(k^2), \quad (\text{A21})$$

$$l_1^s(y) = \frac{M^2}{8\pi^2} \int_0^1 dx \frac{x(1-x)}{M^2(1-x) + m_s^2 x + yx(1-x)}, \quad (\text{A22})$$

$$l_2^s(y) = \frac{1}{16\pi^2} \int_0^1 dx \left[\ln \left[\frac{M^2(1-x) + m_s^2 x + yx(1-x)}{M^2(1-x)^2 + m_s^2 x} \right] + 2M^2 \left[\frac{1-x}{M^2(1-x) + m_s^2 x + yx(1-x)} - \frac{1-x^2}{M^2(1-x)^2 + m_s^2 x} \right] \right], \quad (\text{A23})$$

$$l_1^v(y) = \frac{M^2}{4\pi^2} \int_0^1 dx \frac{x(1-x)}{M^2(1-x) + m_v^2 x + yx(1-x)}, \quad (\text{A24})$$

$$l_2^v(y) = \frac{-1}{4\pi^2} \int_0^1 dx \left[\ln \left[\frac{M^2(1-x) + m_v^2 x + yx(1-x)}{M^2(1-x)^2 + m_v^2 x} \right] + M^2 \left[\frac{2(1-x)}{M^2(1-x) + m_v^2 x + yx(1-x)} - \frac{(1-x)(2-x)}{M^2(1-x)^2 + m_v^2 x} \right] \right]. \quad (\text{A25})$$

APPENDIX B: TWO-LOOP COUNTERTERMS

Here we provide explicit expressions for the scalar two-loop counterterms $\alpha_n^{(2)}$ that appear in Eq. (2.85). The one-loop counterterms $\alpha_n^{(1)}$ are given in Eq. (2.67), and the $\mathcal{O}(\hbar^2)$ counterterms M_c , ξ_N , and γ_s can be determined by applying the renormalization conditions (A10)–(A12) to Eqs. (A5)–(A8). One reason for explicitly defining the two-loop counterterms [rather than simply discarding all divergences through $\mathcal{O}(\phi^4)$ in Eq. (2.85)] is that they will be needed to renormalize divergent subintegrals if one attempts to compute the QHD-I energy density to three-loop order.

To express the counterterms in the most compact form, it is convenient to rewrite Eqs. (2.80) and (2.85) as

$$\mathcal{E}_{\text{VF}}^{(2)}(M^*) = \mathcal{F}(M^*) + \Delta \mathcal{E}_\Sigma(M^*) + \Delta \mathcal{E}_P(M^*) - \sum_{n=1}^4 \frac{1}{n!} \alpha_n^{(2)} \phi^n - \text{VEV}, \quad (\text{B1})$$

where

$$\begin{aligned} \mathcal{F}(M^*) &\equiv \frac{1}{2} g_s^2 \int \frac{d^\tau k}{(2\pi)^4} \frac{d^\tau q}{(2\pi)^4} \text{tr}[G_F^*(k) G_F^*(q)] \Delta^0(k-q) \\ &\quad - \frac{1}{2} g_v^2 \int \frac{d^\tau k}{(2\pi)^4} \frac{d^\tau q}{(2\pi)^4} \text{tr}[\gamma_\mu G_F^*(k) \gamma^\mu G_F^*(q)] D^0(k-q), \end{aligned} \quad (\text{B2})$$

$$\Delta \mathcal{E}_\Sigma(M^*) \equiv i(M_c + \gamma_s \phi) \int \frac{d^\tau k}{(2\pi)^4} \text{tr}[G_F^*(k)] - i \xi_N \int \frac{d^\tau k}{(2\pi)^4} \text{tr}[(\gamma_\mu k^\mu - M) G_F^*(k)], \quad (\text{B3})$$

$$\Delta \mathcal{E}_P(M^*) \equiv -\frac{i}{2} (\alpha_2^{(1)} + \alpha_3^{(1)} \phi + \frac{1}{2} \alpha_4^{(1)} \phi^2) \int \frac{d^\tau k}{(2\pi)^4} \Delta^0(k) - \frac{i}{2} \xi_s \int \frac{d^\tau k}{(2\pi)^4} k^2 \Delta^0(k) - \frac{3i}{2} \xi_v \int \frac{d^\tau k}{(2\pi)^4} k^2 D^0(k), \quad (\text{B4})$$

$$\text{VEV} = \mathcal{F}(M) + \Delta \mathcal{E}_\Sigma(M) + \Delta \mathcal{E}_P(M), \quad (\text{B5})$$

and $\phi = (M - M^*)/g_s$.

With Eq. (2.65), one can expand $\mathcal{F}(M^*)$ as a power series in $(M - M^*)$ and examine the nested, overlapping, and overall divergences in the resulting integral coefficients.⁶⁷ The leading term (which is independent of ϕ) is canceled by the VEV subtraction. Moreover, careful study reveals that $\Delta\mathcal{E}_p(M^*)$ removes the overlapping divergences [which occur through $O(\phi^2)$], and $\Delta\mathcal{E}_\Sigma(M^*)$ removes the nested divergences (which occur to all orders in ϕ). Note that the vector contribution to $\mathcal{F}(M^*)$ contains an overlapping divergence only in the ϕ -independent term, which is explicitly canceled by the VEV subtraction. Thus the $\alpha_n^{(2)}$ counterterms must renormalize only the overall divergences.

The simplest way to define these counterterms is therefore to equate them to the coefficients in the $(M - M^*)$ expansion and use $\Delta\mathcal{E}_\Sigma$ and $\Delta\mathcal{E}_p$ to remove the nested and overlapping divergences from the counterterms themselves. We find

$$\alpha_n^{(2)} \equiv \left[\left[-g_s \frac{\partial}{\partial M^*} \right]^n [\mathcal{F}(M^*) + \Delta\mathcal{E}_\Sigma(M^*)] \right]_{M^*=M} - \frac{i}{2} (\delta_{n1} + \delta_{n2}) \alpha_{n+2}^{(1)} \int \frac{d^\tau k}{(2\pi)^4} \Delta^0(k). \quad (\text{B6})$$

Note that it is important to differentiate $\Delta\mathcal{E}_\Sigma(M^*)$ first, before setting $M^*=M$, to include the contributions from γ_s . [One can immediately set $M^*=M$ in $\mathcal{F}(M^*)$ if desired.] It is readily verified that the $\alpha_n^{(2)}$ counterterms contain only overall divergences.

Because of the similarity between many of the subtractions, the most efficient way to arrive at the finite result for $\mathcal{E}_{\text{VF}}^{(2)}(M^*)$ should now be apparent.⁶⁷ Use Eq. (2.65) and the relations in this Appendix to expand *everything* in Eq. (B1) to $O(\phi^4)$, leaving the higher-order contributions expressed in terms of G_F^* . All terms cancel, except for the $O(\phi^5)$ and higher contributions to $\mathcal{F}(M^*)$ and the subtractions $\Delta\mathcal{E}_\Sigma(M^*)$ of corresponding orders in ϕ . The only remaining divergences are nested ones, and these are removed by the $\Delta\mathcal{E}_\Sigma$ subtractions, producing the renormalized baryon self-energy and baryon-scalar vertex inside the integrals. The finite result agrees with Eq. (2.90).

APPENDIX C: ALTERNATIVE RENORMALIZATION SCHEME

Here we outline an alternative method for renormalizing the two-loop calculation. Instead of directly canceling divergences before completing the momentum integrations, one can employ dimensional regularization to represent these divergences as poles in the complex plane of the number of dimensions.⁴⁷ When this is done for both the two-loop contributions to the energy density and the counterterms, the poles cancel, and one can let the number of dimensions go to four. We performed the calculations in this fashion as a check of the method described in Sec. II and Appendixes A and B.

We will not reproduce the entire calculation here, but provide details for the scalar vacuum fluctuation contribution to the energy. The vector vacuum fluctuation

contribution can be computed analogously, and all other terms are simpler to compute. The scalar vacuum fluctuation contribution to the energy is given by the first term on the right-hand side of Eq. (2.85):

$$\mathcal{E}_{\text{VF}}^{s(2)} = \frac{1}{2} g_s^2 \mu^{8-2\tau} \int \frac{d^\tau k}{(2\pi)^\tau} \int \frac{d^\tau q}{(2\pi)^\tau} \text{tr}[G_F^*(k)G_F^*(q)] \times \Delta^0(k-q). \quad (\text{C1})$$

Here we have introduced the (arbitrary) mass μ to preserve the dimensionality of $\mathcal{E}_{\text{VF}}^{s(2)}$. (μ disappears from the final finite results.) By performing a Wick rotation to Euclidean space and using $\text{tr}[\gamma_\mu \gamma_\nu] = -2\tau \delta_{\mu\nu}$ (remember the factor of 2 from the trace over isospin), one obtains

$$\mathcal{E}_{\text{VF}}^{s(2)} = \tau g_s^2 \mu^{8-2\tau} \int \frac{d^\tau k}{(2\pi)^\tau} \int \frac{d^\tau q}{(2\pi)^\tau} \times \frac{M^{*2} - qk}{(q^2 + M^{*2})(k^2 + M^{*2})[(k-q)^2 + m_s^2]}. \quad (\text{C2})$$

After rewriting qk in terms of factors occurring in the denominator, one obtains

$$\mathcal{E}_{\text{VF}}^{s(2)} = \tau g_s^2 \left[\frac{1}{2} I_1^2(M^*) - I_1(m_s)I_1(M^*) + (2M^{*2} - \frac{1}{2}m_s^2)I_2(m_s, M^*) \right], \quad (\text{C3})$$

where

$$I_1(m) \equiv \mu^{4-\tau} \int \frac{d^\tau k}{(2\pi)^\tau} \frac{1}{k^2 + m^2} = \frac{\Gamma(1-\tau/2)}{(4\pi)^{\tau/2}} \left[\frac{\mu^2}{m^2} \right]^{1-\tau/2} \quad (\text{C4})$$

and

$$I_2(m_s, M^*) \equiv \mu^{8-2\tau} \int \frac{d^\tau k}{(2\pi)^\tau} \int \frac{d^\tau q}{(2\pi)^\tau} \times \{ (q^2 + M^{*2})(k^2 + M^{*2}) \times [(k-q)^2 + m_s^2] \}^{-1}. \quad (\text{C5})$$

$I_2(m_s, M^*)$ is similar to a two-loop integral found in scalar field theories and is discussed in several places,^{17,25,29} however, the massless case or the case with three equal masses is usually considered. To further analyze (C5), insert the identity

$$1 \equiv \frac{1}{2\tau} \left[\frac{\partial q_\mu}{\partial q_\mu} + \frac{\partial k_\mu}{\partial k_\mu} \right]$$

and integrate by parts, noting that the surface terms vanish. After some simple algebra, one obtains

$$I_2(m_s, M^*) = \frac{1}{3-\tau} [2M^{*2}I_3(M^*, M^*, m_s) + m_s^2 I_3(m_s, M^*, M^*)], \quad (C6)$$

where

$$I_3(m_1, m_2, m_3) = \frac{\Gamma(2-\tau/2)}{(4\pi)^{\tau/2}} \mu^{8-2\tau} \int_0^1 dx [x(1-x)]^{\tau/2-2} \int \frac{d^\tau q}{(2\pi)^\tau} [(q^2 + m_1^2)^2 (q^2 + \alpha)^{2-\tau/2}]^{-1}, \quad (C8)$$

where

$$\alpha \equiv m_2^2/x + m_3^2/(1-x). \quad (C9)$$

The remaining momentum integration is easily performed after introducing a second Feynman parametrization, yielding (with $\tau \equiv 4 - 2\epsilon$)

$$I_3(m_1, m_2, m_3) = \frac{\Gamma(2\epsilon)}{(4\pi)^4} \int_0^1 dx [x(1-x)]^{-\epsilon} \int_0^1 dy y^{-1+\epsilon(1-y)} \left[\frac{4\pi\mu^2}{m_1^2(1-y) + \alpha y} \right]^{2\epsilon}. \quad (C10)$$

The next step is to make a Laurent expansion around $\epsilon=0$, but first a potential divergence in the y integration must be removed through an integration by parts. The surface term vanishes, and one finds

$$I_3(m_1, m_2, m_3) = -\frac{1}{(4\pi)^4} \frac{\Gamma(2\epsilon)}{\epsilon} \int_0^1 dx [x(1-x)]^{-\epsilon} \int_0^1 dy y^\epsilon \frac{d}{dy} \left[(1-y) \left[\frac{4\pi\mu^2}{m_1^2(1-y) + \alpha y} \right]^{2\epsilon} \right]. \quad (C11)$$

Since $\Gamma(2\epsilon)/\epsilon$ contains a second-order pole as $\epsilon \rightarrow 0$, the integrand must be expanded to order ϵ^2 , producing

$$I_3(m_1, m_2, m_3) = \frac{1}{(4\pi)^4} \frac{\Gamma(2\epsilon)}{\epsilon} \left[1 - \epsilon \left[2 \ln \left[\frac{m_1^2}{4\pi\mu^2} \right] - 1 \right] + \epsilon^2 \left\{ 1 - \frac{\pi^2}{6} + 2 \left[\ln \left[\frac{m_1^2}{4\pi\mu^2} \right] \right]^2 - 2 \ln \left[\frac{m_1^2}{4\pi\mu^2} \right] + 2 \int_0^1 dx \left[\frac{\alpha \ln(\alpha/m_1^2)}{\alpha - m_1^2} + (\alpha - m_1^2) \int_0^1 dy \frac{\ln(y)}{(\alpha - m_1^2)y + m_1^2} \right] \right\} \right]. \quad (C12)$$

The remaining steps in obtaining a finite expression for $\mathcal{G}_{\text{VF}}^{s(2)}$ are conceptually simple, but algebraically tedious. One must recombine the preceding expressions and make a Laurent expansion in powers of ϵ . Then one adds the counterterms discussed in Appendix B, with each counterterm expressed as a Laurent series in powers of ϵ . The resultant renormalized expression contains no $1/\epsilon$ poles, and the limit $\epsilon \rightarrow 0$ can be taken, yielding

$$\begin{aligned} \mathcal{G}_{\text{VF}}^{s(2)} = & \frac{g_s^2 m_s^4}{64\pi^4} \left[\frac{1}{2} \left[\xi^2 L^2 - 4(\xi - \xi_0)^2 - \frac{4}{\xi_0} (\xi - \xi_0)^3 + \frac{1}{3\xi_0^2} (\xi - \xi_0)^4 \right] \right. \\ & - (1 - L_0) \left[\xi^2 L - 2\xi_0(\xi - \xi_0) - 3(\xi - \xi_0)^2 - \frac{2}{3\xi_0} (\xi - \xi_0)^3 + \frac{1}{6\xi_0^2} (\xi - \xi_0)^4 \right] \\ & - \frac{3}{2} [\xi^4 L^2 - 4\xi_0^2(\xi - \xi_0)^2 - 12\xi_0(\xi - \xi_0)^3 - \frac{35}{3}(\xi - \xi_0)^4] \\ & + (7 - 3L_0 + \xi_1) [\xi^4 L - 2\xi_0^3(\xi - \xi_0) - 7\xi_0^2(\xi - \xi_0)^2 - \frac{26}{3}\xi_0(\xi - \xi_0)^3 - \frac{25}{6}(\xi - \xi_0)^4] \\ & - \xi_2(\xi - \xi_0) [\xi^3 L - 2\xi_0^2(\xi - \xi_0) - 5\xi_0(\xi - \xi_0)^2 - \frac{11}{3}(\xi - \xi_0)^3] \\ & + (\xi - \xi_0)^5 \int_0^1 dx \int_0^1 dy xy(1-x)[1-y + \ln(y)] \\ & \times \left[\frac{\frac{1}{2}y + f_1}{(\xi^2 y + f_1)(\xi_0^2 y + f_1)^5} [5(\xi + \xi_0)(\xi_0^2 y - f_1)^2 - 4\xi_0^5 y^2 - 4\xi f_1^2] \right. \\ & \left. + \frac{x^2(4xy + f_2)}{(\xi^2 f_2 + xy)(\xi_0^2 f_2 + xy)^5} [5(\xi + \xi_0)(\xi_0^2 f_2 - xy)^2 - 4\xi_0^5 f_2^2 - 4x^2 y^2 \xi] \right] \Bigg], \quad (C13) \end{aligned}$$

where

$$\begin{aligned}\xi &\equiv \frac{M^*}{m_s}, \quad \xi_0 \equiv \frac{M}{m_s}, \quad L \equiv \ln \left[\frac{\xi^2}{\xi_0^2} \right], \quad L_0 \equiv \ln(\xi_0^2), \\ \zeta_1 &\equiv \frac{1}{\xi_0^4} \left[(4\xi_0^2 - 1)^{3/2} \cos^{-1} \left[\frac{1}{2\xi_0} \right] + (6\xi_0^4 - 6\xi_0^2 + 1) \ln(\xi_0) - 7\xi_0^4 + \xi_0^2 \right], \\ \zeta_2 &\equiv \frac{2}{\xi_0^4} \left[2(4\xi_0^2 - 1)^{1/2} (\xi_0^2 - 1) \cos^{-1} \left[\frac{1}{2\xi_0} \right] + 2(1 - 3\xi_0^2) \ln(\xi_0) - 3\xi_0^4 + 2\xi_0^2 \right], \\ f_1 &\equiv x(1-x)(1-y), \quad \text{and} \quad f_2 \equiv (1-x)(x+y-xy).\end{aligned}\tag{C14}$$

Equation (C13) has been derived assuming that $\xi_0 > \frac{1}{2}$ and $\xi > 0$, and in this case, it gives the same (numerical) results as Eq. (2.93).

- ¹J. D. Walecka, *Ann. Phys. (N.Y.)* **83**, 491 (1974).
²B. D. Serot and J. D. Walecka, *Adv. Nucl. Phys.* **16**, 1 (1986).
³G. Baym and L. P. Kadanoff, *Phys. Rev.* **124**, 287 (1961).
⁴G. Baym, *Phys. Rev.* **127**, 1391 (1962).
⁵W. E. Caswell and A. D. Kennedy, *Phys. Rev. D* **25**, 392 (1982).
⁶J. C. Collins, *Renormalization* (Cambridge University Press, New York, 1984).
⁷S. A. Chin, *Ann. Phys. (N.Y.)* **108**, 301 (1977).
⁸S. A. Chin and J. D. Walecka, *Phys. Lett.* **52B**, 24 (1974).
⁹C. J. Horowitz and B. D. Serot, *Nucl. Phys.* **A368**, 503 (1981).
¹⁰C. J. Horowitz and B. D. Serot, *Phys. Lett.* **140B**, 181 (1984).
¹¹Lattice treatments do exist for theories without asymptotic freedom, such as QED. See, for example, J. B. Kogut, E. Dagotto, and A. Kocić, *Phys. Rev. Lett.* **61**, 2416 (1988).
¹²P. A. M. Dirac, *Phys. Z. Sowjetunion* **3**, 64 (1933).
¹³R. P. Feynman, *Rev. Mod. Phys.* **20**, 367 (1948).
¹⁴F. A. Berezin, *The Method of Second Quantization* (Academic, New York, 1966).
¹⁵C. Itzykson and J. Zuber, *Quantum Field Theory* (McGraw-Hill, New York, 1980).
¹⁶L. D. Faddeev and A. A. Slavnov, *Gauge Fields: Introduction to Quantum Theory* (Benjamin/Cummings, Reading, MA, 1980).
¹⁷P. Ramond, *Field Theory: A Modern Primer* (Benjamin, Reading, MA, 1981).
¹⁸K. Huang, *Quarks, Leptons, and Gauge Fields* (World Scientific, Singapore, 1982).
¹⁹J. Schwinger, *Proc. Nat. Acad. Sci. (U.S.A.)* **37**, 452 (1951); **37**, 455 (1951).
²⁰G. Jona-Lasinio, *Nuovo Cimento* **34**, 1790 (1964).
²¹Y. Nambu, *Phys. Lett.* **26B**, 626 (1968).
²²S. Coleman and E. Weinberg, *Phys. Rev. D* **7**, 1888 (1973).
²³R. Jackiw, *Phys. Rev. D* **9**, 1686 (1974).
²⁴J. M. Cornwall, R. Jackiw, and E. Tomboulis, *Phys. Rev. D* **10**, 2428 (1974).
²⁵J. Iliopoulos, C. Itzykson, and A. Martin, *Rev. Mod. Phys.* **47**, 165 (1975).
²⁶S. Coleman, in *Laws of Hadronic Matter*, Proceedings of the 11th Course of the International School in Physics "Ettore Majorana," edited by A. Zichichi (Academic, New York, 1975).
²⁷S. Coleman, in *New Phenomena in Subnuclear Physics*, edited by A. Zichichi (Plenum, New York, 1977).
²⁸T. D. Lee and G. C. Wick, *Phys. Rev. D* **9**, 2291 (1974).
²⁹R. J. Perry, Ph.D. thesis, University of Maryland, 1984.
³⁰R. J. Perry, in *Proceedings of the International Conference on Spin Observables of Nuclear Probes*, edited by C. J. Horowitz, C. D. Goodman, and G. E. Walker (Plenum, New York, 1989).
³¹R. J. Perry and D. A. Wasson, in *Nuclear and Particle Physics on the Light Cone*, edited by M. B. Johnson and L. S. Kisslinger (World Scientific, Singapore, 1989).
³²T. D. Lee and M. Margulies, *Phys. Rev. D* **11**, 1591 (1975).
³³M. Margulies, *Phys. Rev. D* **13**, 1621 (1976); **13**, 1642 (1976).
³⁴E. M. Nyman and M. Rho, *Phys. Lett.* **60B**, 134 (1976).
³⁵E. M. Nyman and M. Rho, *Nucl. Phys.* **A268**, 408 (1976).
³⁶A. D. Jackson, M. Rho, and E. Krotscheck, *Nucl. Phys.* **A407**, 495 (1983).
³⁷I. A. Akhiezer and S. V. Peletminskii, *Zh. Eksp. Teor. Fiz.* **11**, 1829 (1960) [*Sov. Phys.—JETP* **11**, 1316 (1960)].
³⁸R. J. Furnstahl and B. D. Serot, *Ann. Phys. (N.Y.)* **185**, 138 (1988).
³⁹N. P. Landsman and Ch. G. van Weert, *Phys. Rep.* **145**, 141 (1987).
⁴⁰I. J. R. Aitchison and C. M. Fraser, *Phys. Lett.* **146B**, 63 (1984).
⁴¹L. H. Chan, *Phys. Rev. Lett.* **54**, 1222 (1985); **55**, 21 (1985); **56**, 404(E) (1986).
⁴²O. Cheyette, *Phys. Rev. Lett.* **55**, 2394 (1985).
⁴³C. M. Fraser, *Z. Phys. C* **28**, 101 (1985).
⁴⁴R. J. Perry, *Phys. Lett. B* **182**, 269 (1986).
⁴⁵R. A. Freedman, *Phys. Lett.* **71B**, 369 (1977).
⁴⁶R. J. Furnstahl and B. D. Serot (unpublished).
⁴⁷G. 't Hooft and M. Veltman, *Nucl. Phys.* **B44**, 189 (1972).
⁴⁸Here the symmetry of the integrand has been invoked to discard a term proportional to the baryon density of the vacuum. The same result is achieved by normal ordering the vector-baryon interaction in the Lagrangian (2.42).
⁴⁹M. Jaminon, C. Mahaux, and P. Rochus, *Nucl. Phys.* **A365**, 371 (1981).
⁵⁰C. J. Horowitz and B. D. Serot, *Phys. Lett.* **108B**, 377 (1982).
⁵¹C. J. Horowitz and B. D. Serot, *Phys. Lett.* **109B**, 341 (1982).
⁵²C. J. Horowitz and B. D. Serot, *Nucl. Phys.* **A399**, 529 (1983).
⁵³A. Bouyssy, J.-F. Mathiot, N. Van Giai, and S. Marcos, *Phys. Rev. C* **36**, 380 (1987).
⁵⁴R. J. Furnstahl and C. J. Horowitz, *Nucl. Phys.* **A485**, 632 (1988).
⁵⁵While this renormalization procedure produces the simplest expression for the energy density, it will nevertheless lead to a shift in the pole of the vector propagator from its tree-level value. The pole position can be restored by including a *finite* counterterm of the form $\delta m_v^2 V_\mu V^\mu$. We will use the simpler procedure in this work.
⁵⁶W. Zimmerman, *Ann. Phys. (N.Y.)* **77**, 536 (1973).
⁵⁷As noted above, this mass parameter will not correspond to

- the pole in the vector meson propagator at the two-loop level.
- ⁵⁸The scalar mass in this parameter set was fitted using the experimental charge radius of ^{40}Ca as an additional input; however, the one-loop energy in nuclear matter depends only on the ratios of meson couplings to masses in this model.
- ⁵⁹R. Machleidt, K. Holinde, and Ch. Elster, *Phys. Rep.* **149**, 1 (1987).
- ⁶⁰The results presented here are not changed significantly if moderate variations of the vector meson mass are also allowed.
- ⁶¹Note that the Yukawa potentials for sets *A* and *B* in Fig. 9 are *not* equivalent to the *NN* interaction obtained from the two-loop effective action. Our renormalization prescription ensures that meson exchange at zero momentum transfer (as in nuclear matter) is unchanged by the loop corrections; however, the *NN* interaction also contains momentum components affected by loop corrections.
- ⁶²T. L. Ainsworth, G. E. Brown, M. Prakash, and W. Weise, *Phys. Lett. B* **200**, 413 (1988).
- ⁶³A. K. Kerman and L. D. Miller, *Field Theory Methods for Finite Nuclear Systems and the Possibility of Density Isomerism*, MIT-CTP Report No. 449, 1974.
- ⁶⁴T. Matsui and B. D. Serot, *Ann. Phys. (N.Y.)* **144**, 107 (1982).
- ⁶⁵Remember, however, that some of our renormalization conditions are specified at zero density. The loop expansion might succeed as a high-density expansion if a high-density renormalization scheme is used.
- ⁶⁶J. D. Bjorken and S. D. Drell, *Relativistic Quantum Fields* (McGraw-Hill, New York, 1965).
- ⁶⁷A. F. Bielajew, private communication.
- ⁶⁸The discussion of Euclidean momenta in Sec. 6-2-4 of Ref. 15 is applicable to Eq. (2.90) because all the external momenta are zero.